Dynamical description of partonic phase at finite chemical potential

Elena Bratkovskaya

(GSI Darmstadt & Uni. Frankfurt)

Pierre Moreau, Olga Soloveva, Lucia Oliva, Taesoo Song, Wolfgang Cassing

The ‚holy grail‘ of heavy-ion physics:

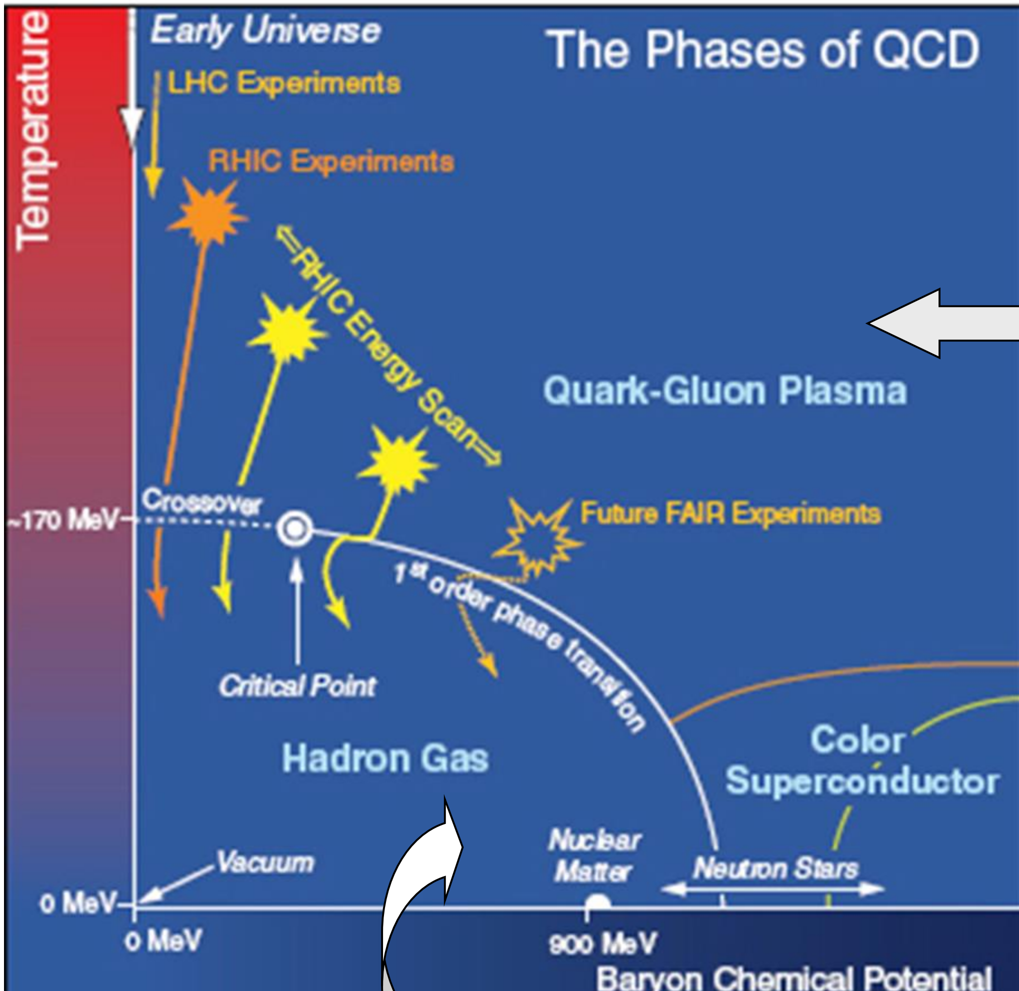

The phase diagram of QCD

- Study of the phase transition from hadronic to partonic matter – Quark-Gluon-Plasma

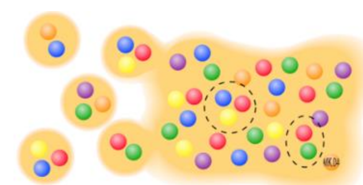

- Search for the critical point
- Search for signatures of chiral symmetry restoration
- Study of the in-medium properties of hadrons at high baryon density and temperature

Theory: lattice QCD data for $\mu_B = 0$ and finite $\mu_B > 0$

- Deconfinement phase transition from hadron gas to QGP with increasing T and μ_B

lQCD: J. Guenther et al., Nucl. Phys. A 967 (2017) 720

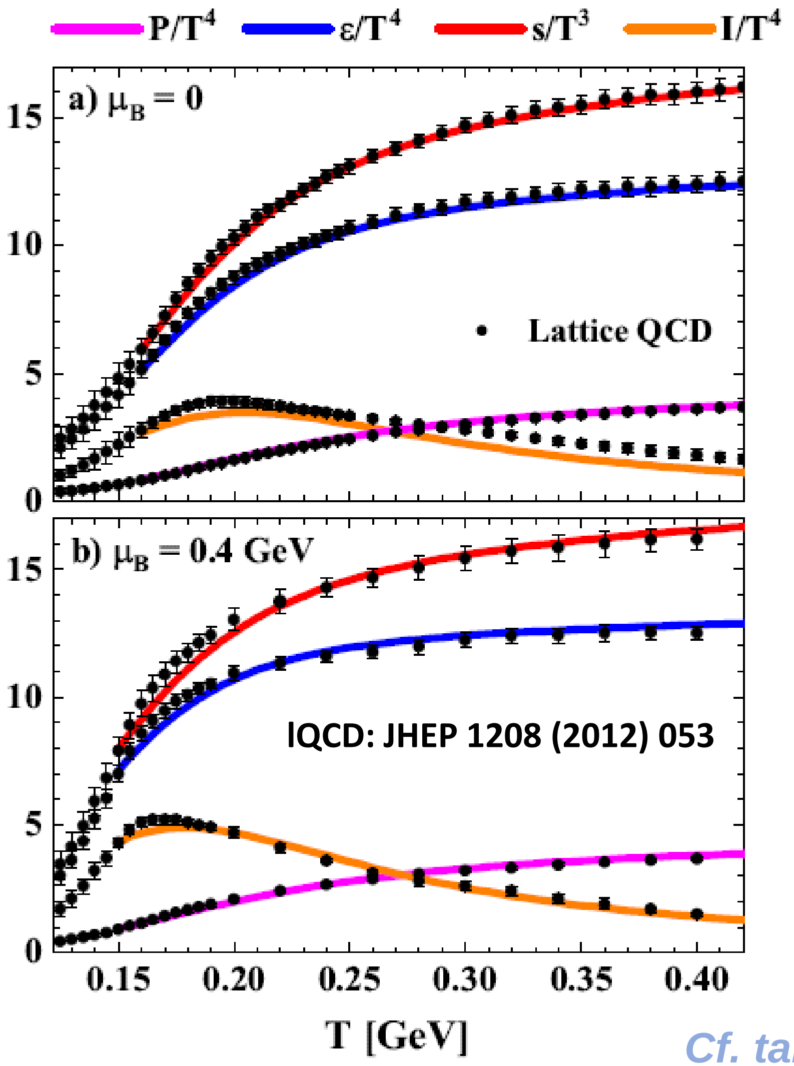

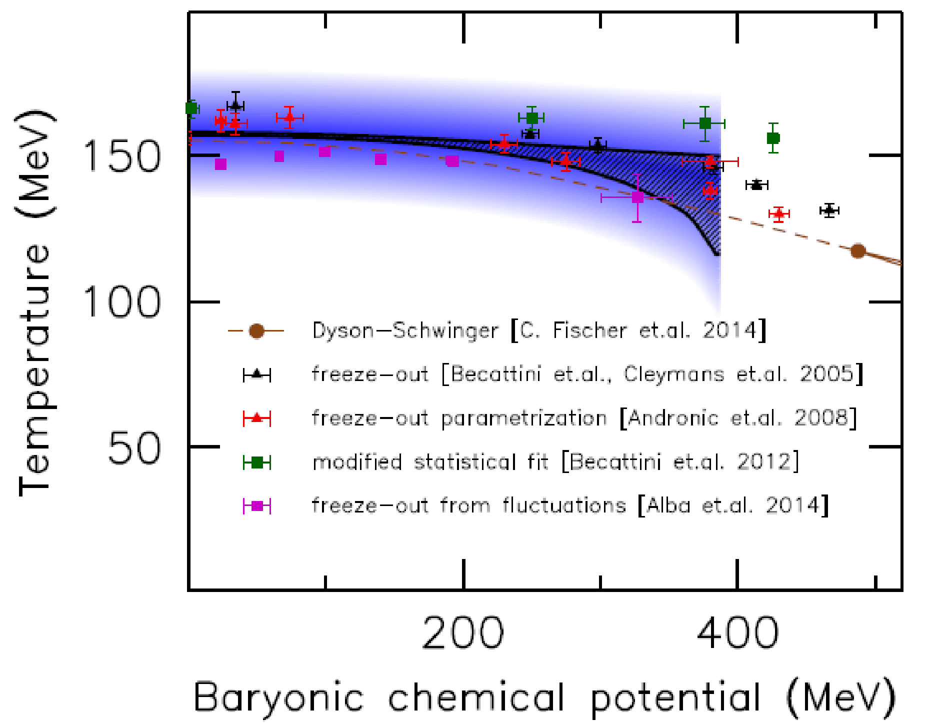

➔ Lattice QCD results: up to $\mu_B < 400\ MeV$:
Crossover: hadron gas → QGP

Cf. talk by Claudia Ratti

Degrees-of-freedom of QGP

❖ lQCD gives QGP EoS at finite μ_B

! need to be interpreted in terms of degrees-of-freedom

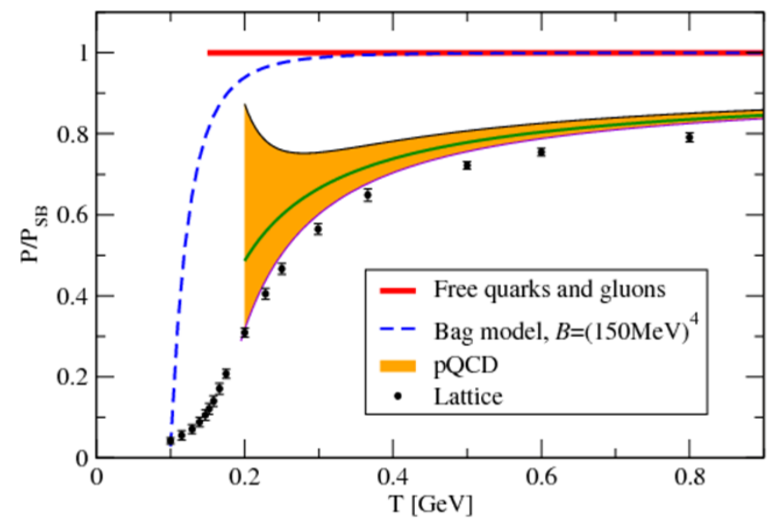

Non-perturbative QCD ← pQCD

pQCD:

- weakly interacting system
- massless quarks and gluons

Thermal QCD

= QCD at high parton densities:

- strongly interacting system
- massive quarks and gluons

➔ quasiparticles

= effective degrees-of-freedom

❖ How to learn about degrees-of-freedom of QGP ? ➔ HIC experiments

DQPM (T, μ_q)

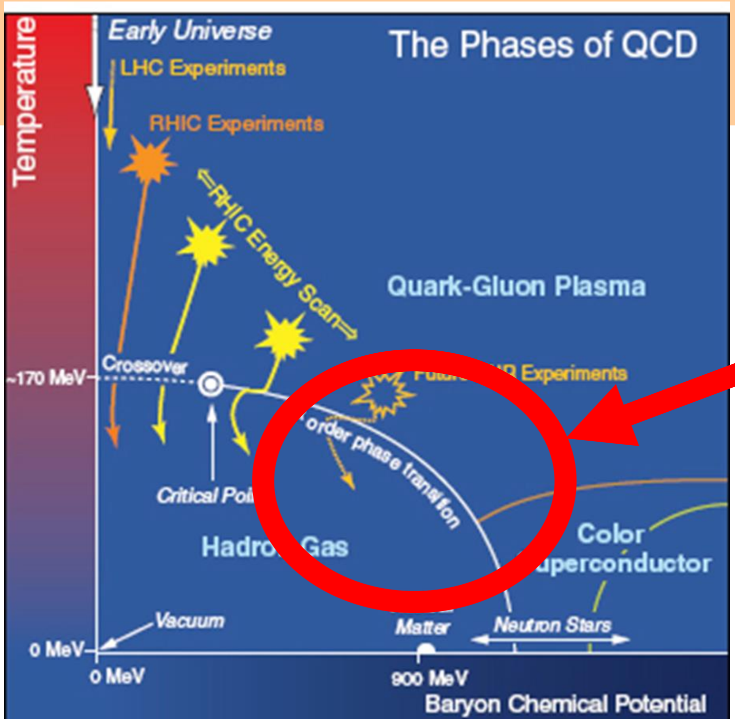

finite μ_q

Dynamical QuasiParticle Model (DQPM)

- The QGP phase is described in terms of **interacting quasiparticles: quarks and gluons** with Lorentzian spectral functions:

$$\rho_j(\omega,\mathbf{p}) = \frac{\gamma_j}{\tilde{E}_j}\left(\frac{1}{(\omega-\tilde{E}_j)^2+\gamma_j^2} - \frac{1}{(\omega+\tilde{E}_j)^2+\gamma_j^2}\right)$$

$$\equiv \frac{4\omega\gamma_j}{\left(\omega^2-\mathbf{p}^2-M_j^2\right)^2+4\gamma_j^2\omega^2}$$

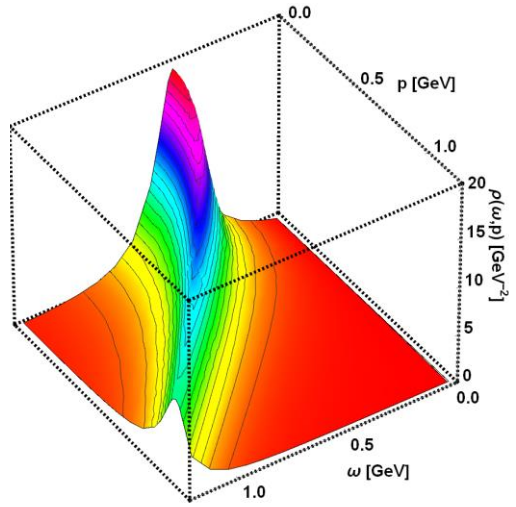

- Resummed properties of the quasiparticles are specified by scalar **complex self-energies:**

gluon propagator: $\Delta^{-1} = P^2 - \Pi$	&	quark propagator $S_q^{-1} = P^2 - \Sigma_q$
gluon self-energy: $\Pi = M_g^2 - i2g_g\omega$	&	quark self-energy: $\Sigma_q = M_q^2 - i2g_q\omega$

- Real part of the self-energy: thermal mass (M_g, M_q)
- Imaginary part of the self-energy: interaction width of partons (γ_g, γ_q)

Peshier, Cassing, PRL 94 (2005) 172301; Cassing, NPA 791 (2007) 365: NPA 793 (2007)

Parton properties

- Modeling of the quark/gluon masses and widths (inspired by HTL calculations)

Masses:

$$M^2_{q(\bar{q})}(T,\mu_B) = \frac{N_c^2-1}{8N_c} g^2(T,\mu_B) \left(T^2 + \frac{\mu_q^2}{\pi^2}\right)$$

$$M^2_g(T,\mu_B) = \frac{g^2(T,\mu_B)}{6}\left(\left(N_c + \frac{1}{2}N_f\right)T^2 + \frac{N_c}{2}\sum_q \frac{\mu_q^2}{\pi^2}\right)$$

Widths:

$$\gamma_{q(\bar{q})}(T,\mu_B) = \frac{1}{3}\frac{N_c^2-1}{2N_c}\frac{g^2(T,\mu_B)T}{8\pi}\ln\left(\frac{2c}{g^2(T,\mu_B)}+1\right)$$

$$\gamma_g(T,\mu_B) = \frac{1}{3}N_c\frac{g^2(T,\mu_B)T}{8\pi}\ln\left(\frac{2c}{g^2(T,\mu_B)}+1\right)$$

→ **DQPM :**
only one parameter (c = 14.4) + (T,μ_B)- dependent coupling constant have to be determined from lattice results

- **Coupling constant:** input: lQCD entropy density as a function of temperature for μ_B
  → Fit to lattice data at μ_B=0 with

$$g^2(s/s_{SB}) = d\left((s/s_{SB})^e - 1\right)^f$$

$$s_{SB}^{QCD} = 19/9\pi^2T^3$$

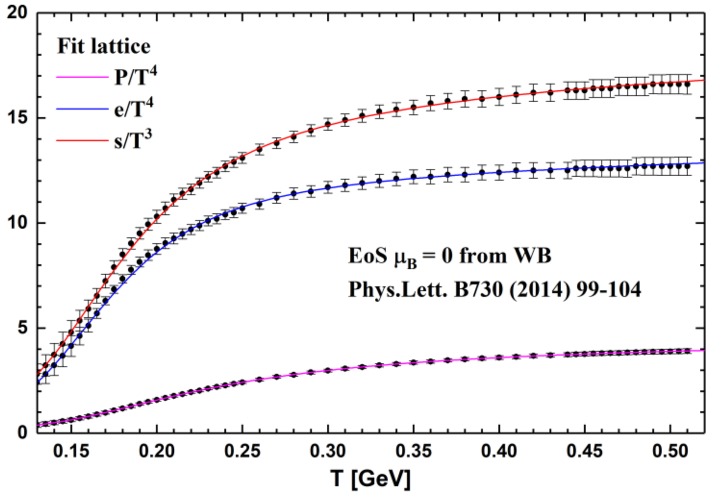

H. Berrehrah et al, PRC 93 (2016) 044914,
Int.J.Mod.Phys. E25 (2016) 1642003,

DQPM at finite (T, μ_q): scaling hypothesis

- **Scaling hypothesis for the effective temperature T***
  for $N_f = N_c = 3$

$$\mu_u = \mu_d = \mu_s = \mu_q \qquad T^{*2} = T^2 + \frac{\mu_q^2}{\pi^2}$$

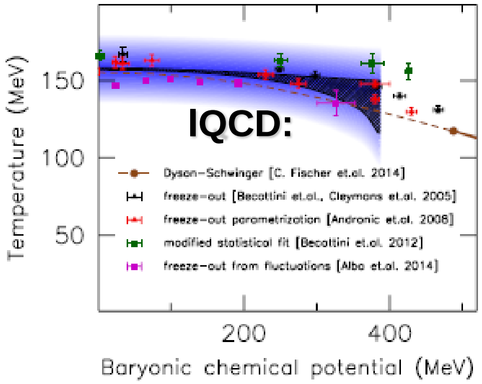

- **Coupling constant:**

$$g(T/T_c(\mu=0)) \longrightarrow g(T^\star/T_c(\mu))$$

- **Critical temperature $T_c(\mu_q)$:**
  obtained by requiring a constant energy density ε for the system at $T=T_c(\mu_q)$ where ε at $T_c(\mu_q=0)$=156 GeV is fixed by lQCD at μ_q=0

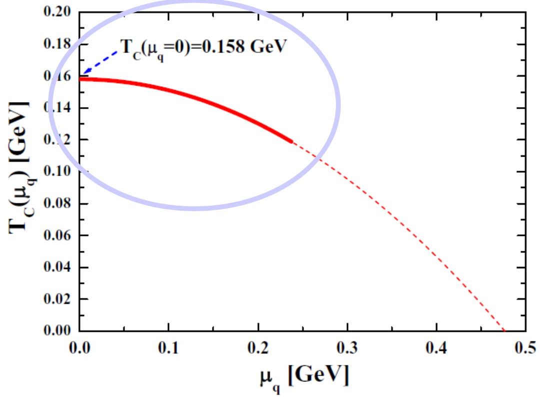

$$\frac{T_c(\mu_q)}{T_c(\mu_q=0)} = \sqrt{1-\alpha\,\mu_q^2} \approx 1-\alpha/2\,\mu_q^2 + \cdots$$

$$\alpha \approx 8.79\ \text{GeV}^{-2}$$

! Consistent with lattice QCD:

lQCD: C. Bonati et al., PRC90 (2014) 114025

$$\frac{T_c(\mu_B)}{T_c} = 1 - \kappa\left(\frac{\mu_B}{T_c}\right)^2 + \cdots$$

lQCD $\kappa = 0.013(2)$ ⟷ $\kappa_{DQPM} \approx 0.0122$

H. Berrehrah et al, PRC 93 (2016) 044914, Int.J.Mod.Phys. E25 (2016) 1642003,

DQPM: parton properties

- Coupling constant as a function of (T, μ_B)

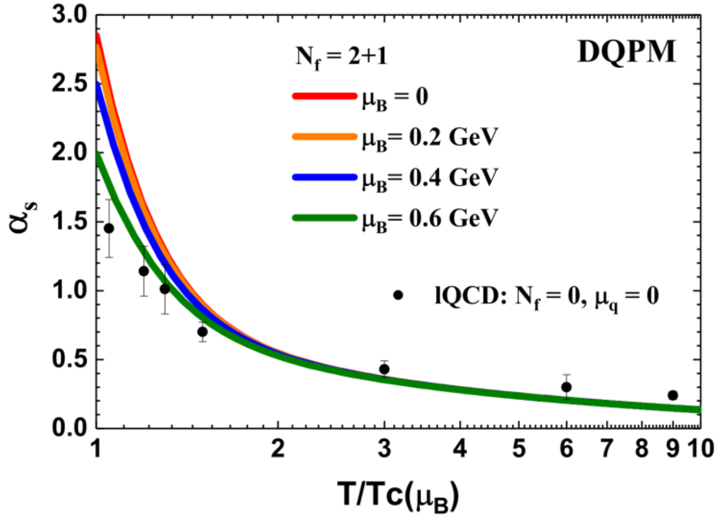

➔ **Lorentzian spectral function:**

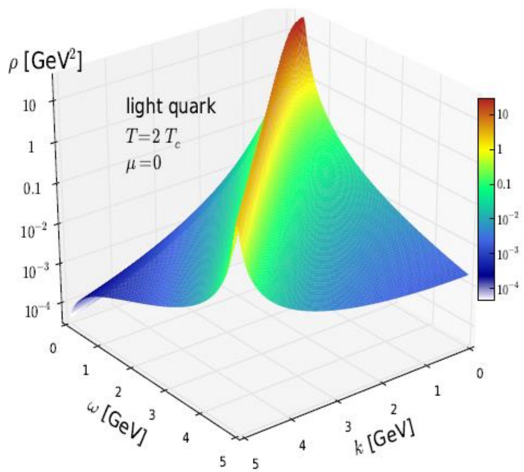

- Masses and widths as a function of (T, μ_B)

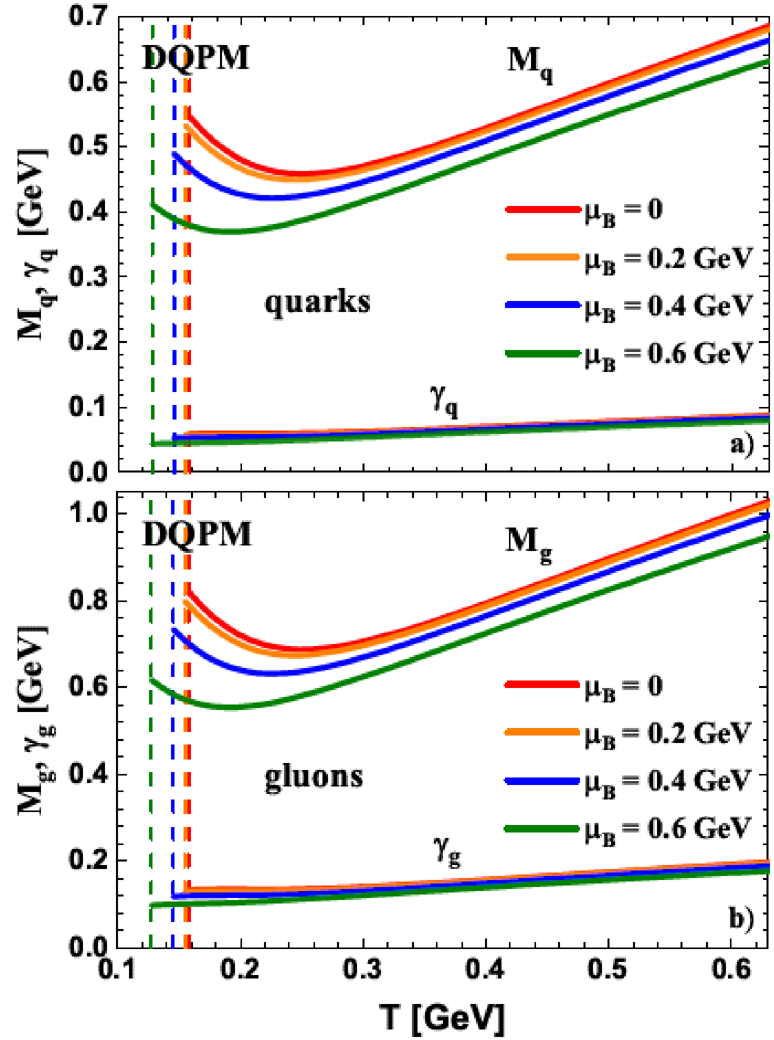

P. Moreau et al., arXiv:1903.10257, PRC (2019)

DQPM Thermodynamics

- **Entropy and baryon density** in the quasiparticle limit (G. Baym 1998):

$$s^{dqp} = - \int \frac{d\omega}{2\pi}\frac{d^3p}{(2\pi)^3}\left[d_g \frac{\partial n_B}{\partial T}\left(\mathrm{Im}(\ln -\Delta^{-1}) + \mathrm{Im}\,\Pi\,\mathrm{Re}\,\Delta\right) + \sum_{q=u,d,s} d_q \frac{\partial n_F(\omega-\mu_q)}{\partial T}\left(\mathrm{Im}(\ln -S_q^{-1}) + \mathrm{Im}\,\Sigma_q\,\mathrm{Re}\,S_q\right) + \sum_{\bar q=\bar u,\bar d,\bar s} d_{\bar q} \frac{\partial n_F(\omega+\mu_q)}{\partial T}\left(\mathrm{Im}(\ln -S_{\bar q}^{-1}) + \mathrm{Im}\,\Sigma_{\bar q}\,\mathrm{Re}\,S_{\bar q}\right)\right]$$

$$n^{dqp} = - \int \frac{d\omega}{2\pi}\frac{d^3p}{(2\pi)^3}\left[\sum_{q=u,d,s} d_q \frac{\partial n_F(\omega-\mu_q)}{\partial \mu_q}\left(\mathrm{Im}(\ln -S_q^{-1}) + \mathrm{Im}\,\Sigma_q\,\mathrm{Re}\,S_q\right) + \sum_{\bar q=\bar u,\bar d,\bar s} d_{\bar q} \frac{\partial n_F(\omega+\mu_q)}{\partial \mu_q}\left(\mathrm{Im}(\ln -S_{\bar q}^{-1}) + \mathrm{Im}\,\Sigma_{\bar q}\,\mathrm{Re}\,S_{\bar q}\right)\right]$$

Blaizot, Iancu, Rebhan, Phys. Rev. D 63 (2001) 065003

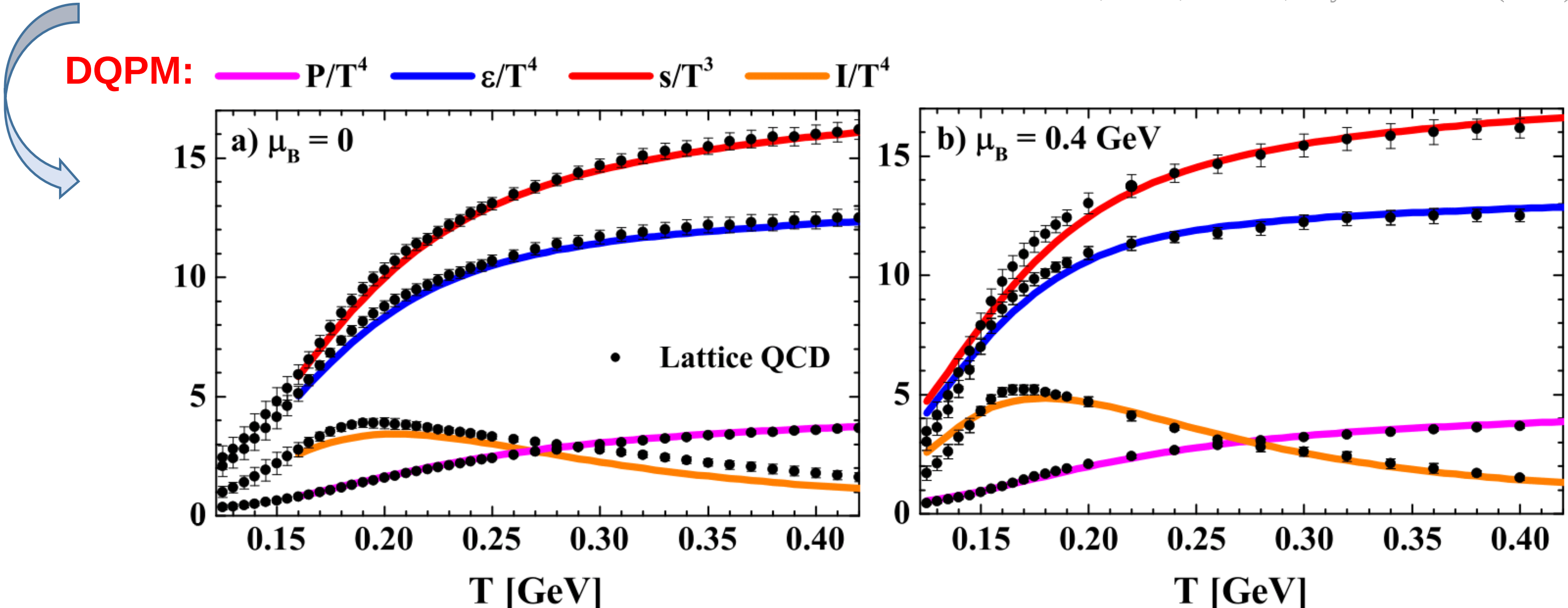

lQCD: JHEP 1208 (2012) 053

DQPM EoS at finite (T, μ_B)

Taylor series of thermodynamic quantities in terms of (μ_B/T)

- For the pressure:

$$\frac{P(T,\mu_B)}{T^4} = \sum_{n=0} \frac{1}{n!} \chi_B^n \left(\frac{\mu_B}{T}\right)^n$$

with the baryon number susceptibilities defined as:

$$\chi_B^n = \left. \frac{\partial^n P}{\partial \mu_B^n} \right|_{\mu_B=0}$$

Cf. talk by Claudia Ratti

- Recent lQCD results - with the 6th order susceptibility

$$\frac{P}{T^4} = c_0(T) + c_2(T)\left(\frac{\mu_B}{T}\right)^2 + c_4(T)\left(\frac{\mu_B}{T}\right)^4 + c_6(T)\left(\frac{\mu_B}{T}\right)^6 + \mathcal{O}\left(\mu_B^8\right)$$

WB lQCD: J. Günther, R. Bellwied, S. Borsanyi, Z. Fodor, S. D. Katz, A. Pasztor, C. Ratti, EPJ Web Conf. 137, 07008 (2017) 158

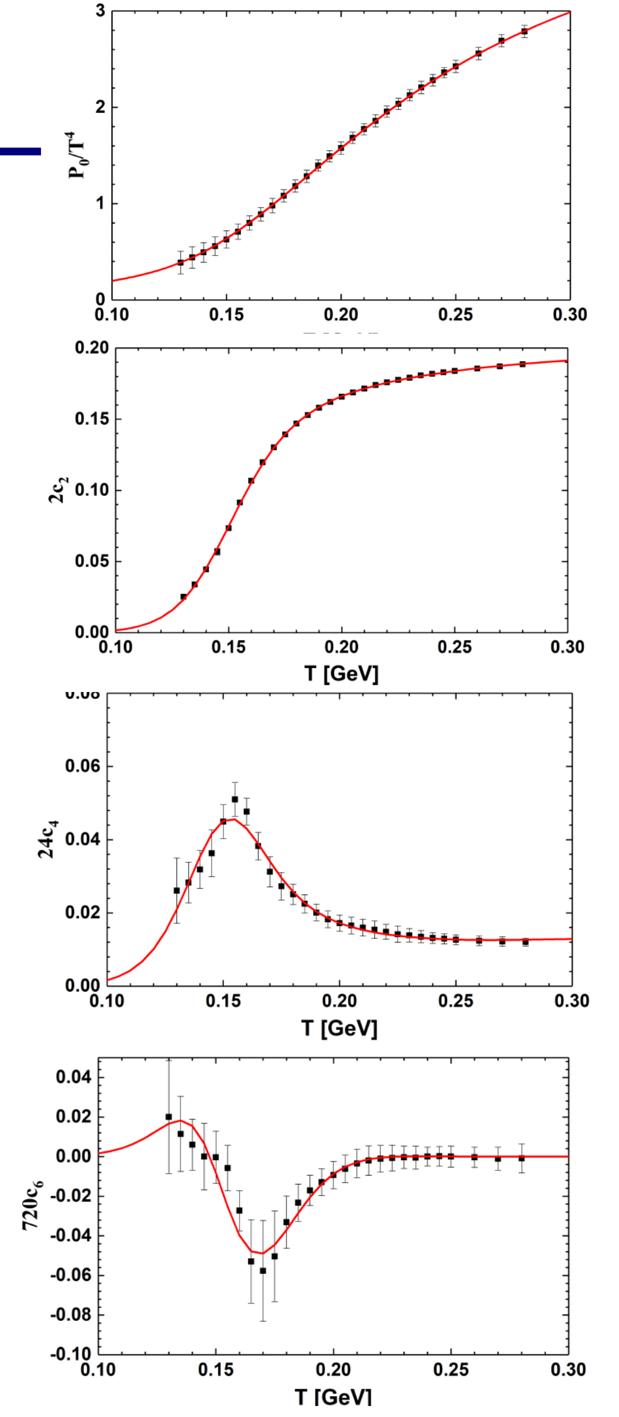

DQPM: Isentropic trajectories for (T, μ_B)

- Correspondance $s/n_B \leftrightarrow$ collisional energy

s/n_B = 420 ↔ 200 GeV
= 144 ↔ 62.4 GeV
= 94 ↔ 39 GeV
= 70 ↔ 27 GeV
= 51 ↔ 19.6 GeV
= 30 ↔ 14.5 GeV

DQPM

- Safe for $(\mu_B/T) < 2$

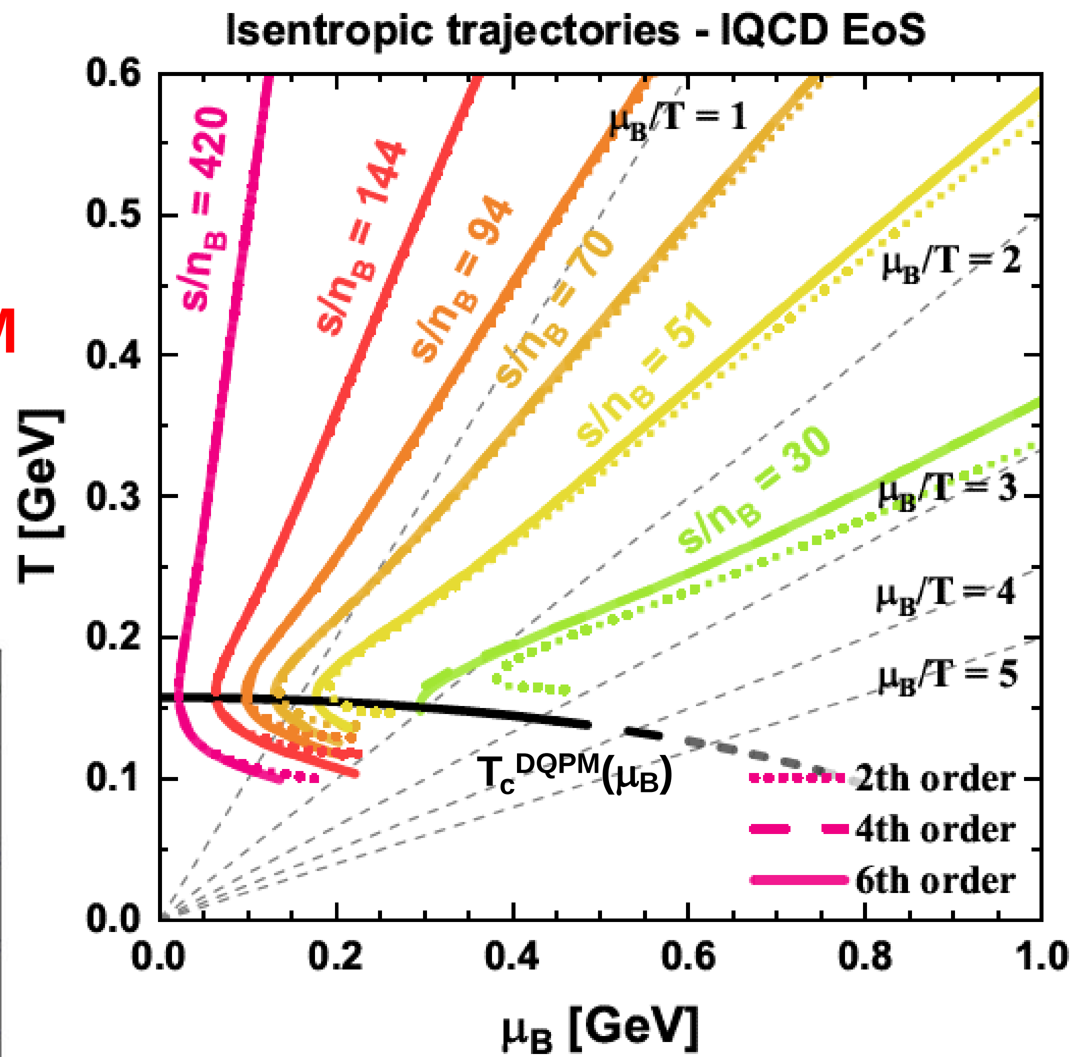

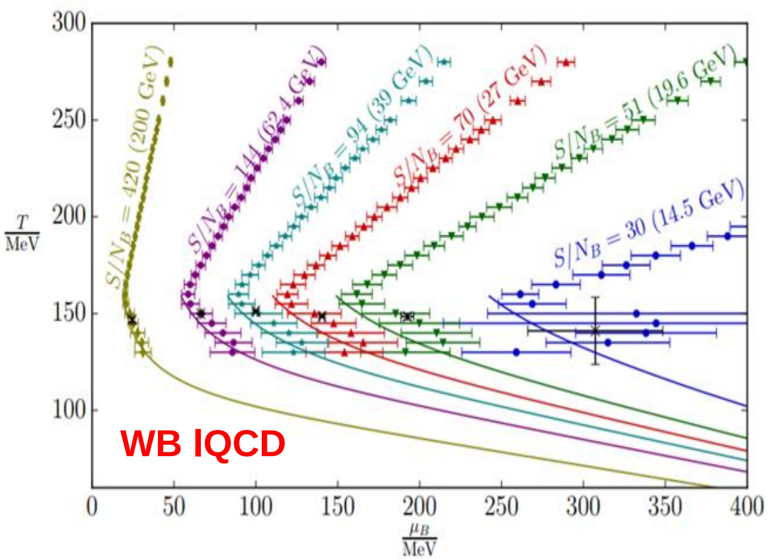

P. Moreau et al., arXiv:1903.10257, PRC (2019)

lQCD: WB, PoS CPOD2017 (2018) 032

QGP in DQPM:
partonic interactions

Partonic interactions

Reminder (2013): DQPM(T) in PHSD 4.0

DQPM provides the total width Γ of the dynamical quasiparticles

$$\Gamma_{total} = \Gamma_{elastic} + \Gamma_{inelastic}$$

V. Ozvenchuk et al., PRC 87 (2013) 024901, PRC 87 (2013) 064903

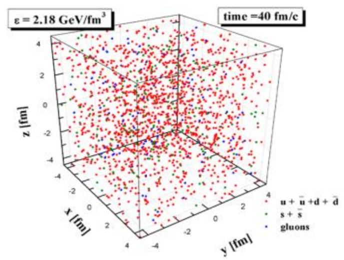

- **obtain the partial widths (i.e. cross sections) for different channels from the PHSD simulations in the box: transition rates ←→ DQPM width**

- **(quasi-) elastic collisions:**

$$q+q \rightarrow q+q \qquad g+q \rightarrow g+q$$
$$q+\bar{q} \rightarrow q+\bar{q} \qquad g+\bar{q} \rightarrow g+\bar{q}$$
$$\bar{q}+\bar{q} \rightarrow \bar{q}+\bar{q} \qquad g+g \rightarrow g+g$$

→ $\sigma_i\,(\varepsilon)$

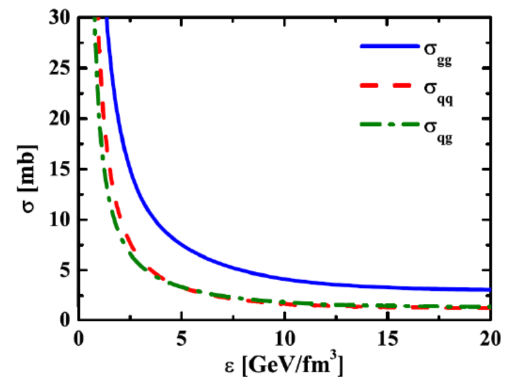

- **inelastic collisions:**

$$q+\bar{q} \rightarrow g \qquad q+\bar{q} \rightarrow g+g$$
$$g \rightarrow q+\bar{q} \qquad g \rightarrow g+g$$

→ $$\sigma_{q\bar{q}\rightarrow g}(s,\varepsilon,M_q,M_{\bar{q}}) = \frac{2}{4}\frac{4\pi s\Gamma_g^2(\varepsilon)}{\left[s-M_g^2(\varepsilon)\right]^2+s\Gamma_g^2(\varepsilon)}\frac{1}{P_{\rm rel}^2}$$

2016-2019 →

To improve the description of QGP dynamics in PHSD we need:
off-shell differential and total cross sections $\sigma_i\,(s,m_1,m_2,T,\mu_q)$
for all combinations *i* =(flavor, spin, color)

PHSD 5.0

H. Berrehrah et al, PRC 93 (2016) 044914, Int.J.Mod.Phys. E25 (2016) 1642003, → **P. Moreau et al., arXiv:1903.10257, PRC (2019)**

Partonic interactions: matrix elements

DQPM partonic cross sections → leading order diagrams

- **Propagators for massive bosons and fermions:**

$$= -i\delta_{ab}\frac{g^{\mu\nu} - q^\mu q^\nu / M_g^2}{q^2 - M_g^2 + 2i\gamma_g q_0}$$

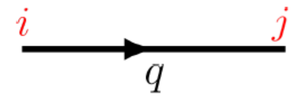

$$= i\delta_{ij}\frac{\not{q} + M_q}{q^2 - M_q^2 + 2i\gamma_q q_0}$$

qq' → qq' scattering

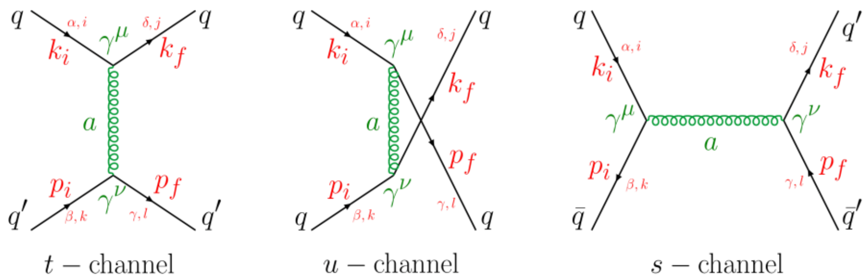

gq → gq scattering

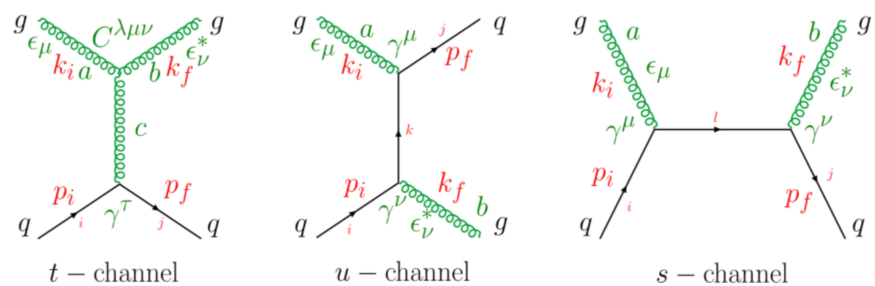

gg→ gg scattering

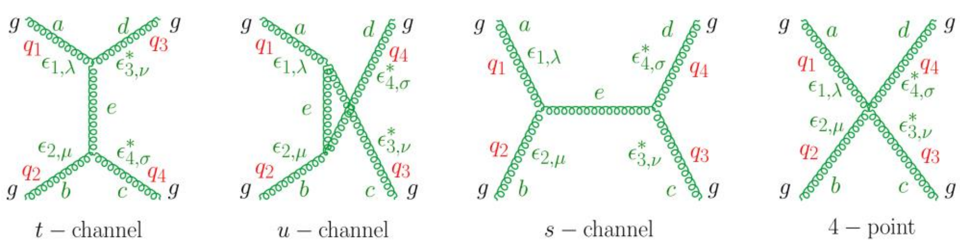

H. Berrehrah et al, PRC 93 (2016) 044914, Int.J.Mod.Phys. E25 (2016) 1642003, → **P. Moreau et al., arXiv:1903.10257, PRC (2019)**

Differential cross section

- On-shell:

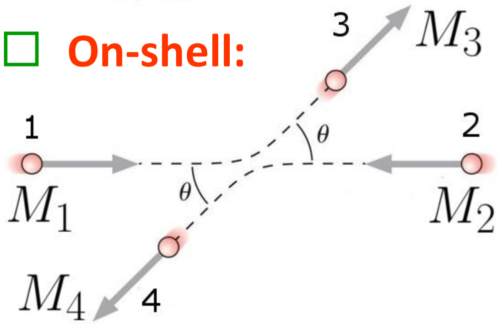

Initial masses: pole masses
Final masses: pole masses

- Off-shell:

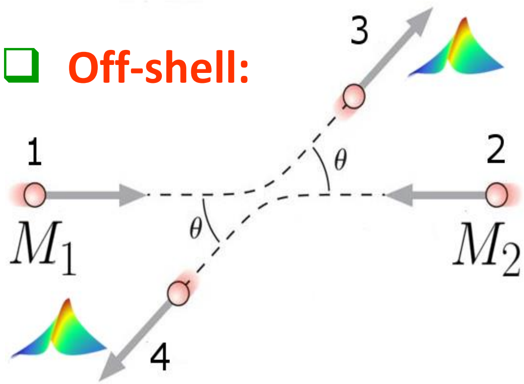

Initial masses: pole masses
Final masses: integrated over spectral functions

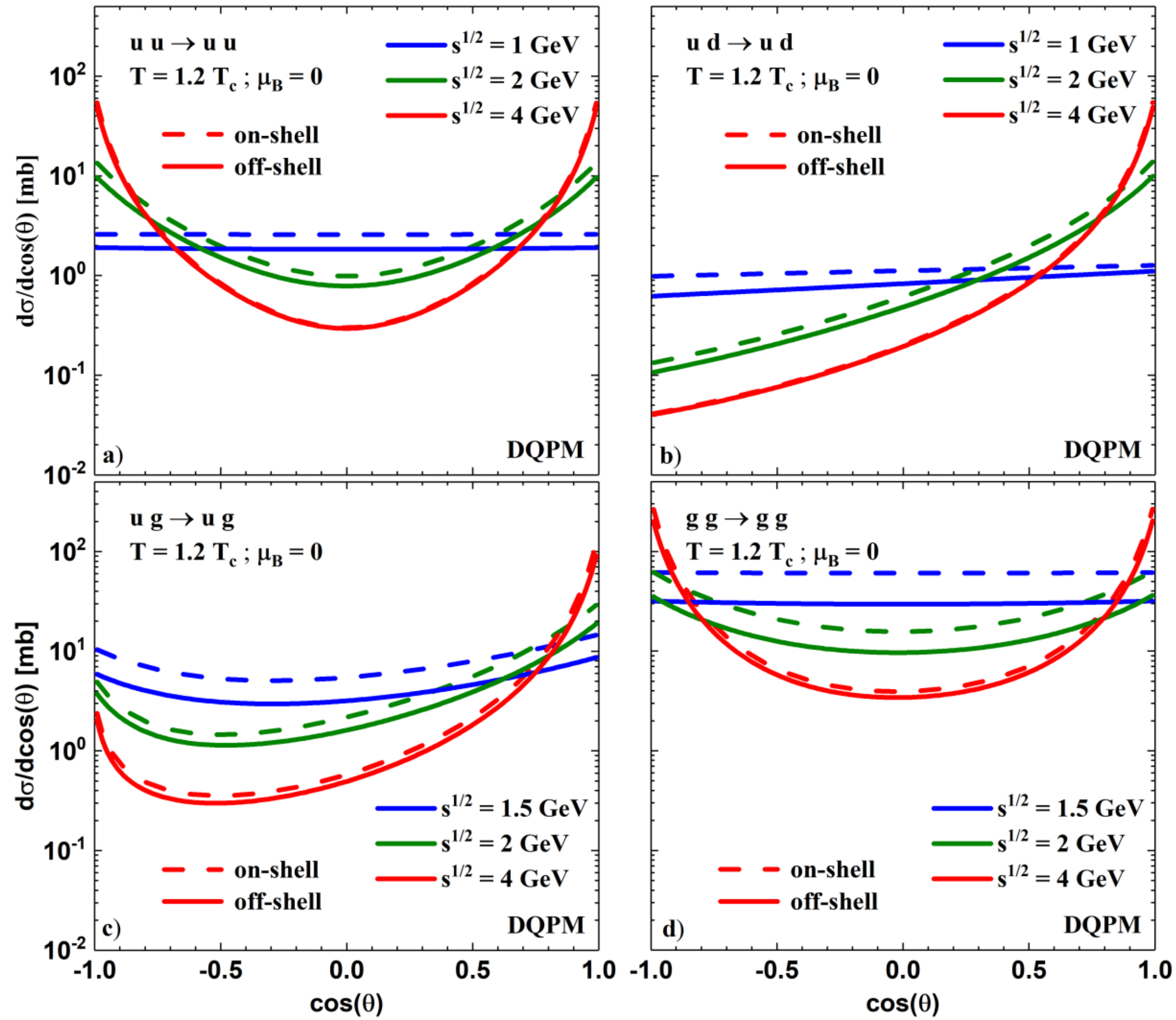

- **At lower s: off-shell σ < on -shell σ since $\omega_3 + \ \omega_4 < \sqrt{s}$**

P. Moreau et al., arXiv:1903.10257, PRC (2019)

DQPM (T, μ_q) :
transport properties at finite (T, μ_q)

Off-shell collision rate

$$\Gamma_i^{\rm off}(T,\mu_q) = \frac{d_i}{n_i^{\rm off}(T,\mu_q)} \int \frac{d^4p_i}{(2\pi)^4}\ \theta(\omega_i)\ \tilde{\rho}_i\ f_i(\omega_i,T,\mu_q)$$
$$\times \sum_{j=q,\bar{q},g} \int \frac{d^4p_j}{(2\pi)^4}\ \theta(\omega_j)\ d_j\ \tilde{\rho}_j\ f_j$$
$$\times \int \frac{d^4p_3}{(2\pi)^4}\ \theta(\omega_3)\ \tilde{\rho}_3 \int \frac{d^4p_4}{(2\pi)^4}\ \theta(\omega_4)\ \tilde{\rho}_4 (1\pm f_3)(1\pm f_4)$$
$$\times |\bar{\mathcal{M}}|^2(p_i,p_j,p_3,p_4)\,(2\pi)^4\delta^{(4)}\left(p_i+p_j-p_3-p_4\right),$$

- **off-shell density**

$$n_i^{\rm off}(T,\mu_q) = d_i \int \frac{d^4p_i}{(2\pi)^4}\ \theta(\omega_i)\ 2\omega_i\ \tilde{\rho}_i\ f_i(T,\mu_q)$$

- **renormalized spectral-function for the time-like sector**

$$\tilde{\rho}_j(\omega_j,\mathbf{p}_j) = \frac{\rho(\omega_j,\mathbf{p}_j)\ \theta(p_j^2)}{\int_0^\infty \frac{d\omega_j}{(2\pi)}\ 2\omega_j\ \rho(\omega_j,\mathbf{p}_j)\ \theta(p_j^2)}$$

normalized to 1 and

$$\lim_{\gamma_j\to 0} \rho_j(\omega,\mathbf{p}) = 2\pi\ \delta(\omega^2-\mathbf{p}^2-M_j^2)$$

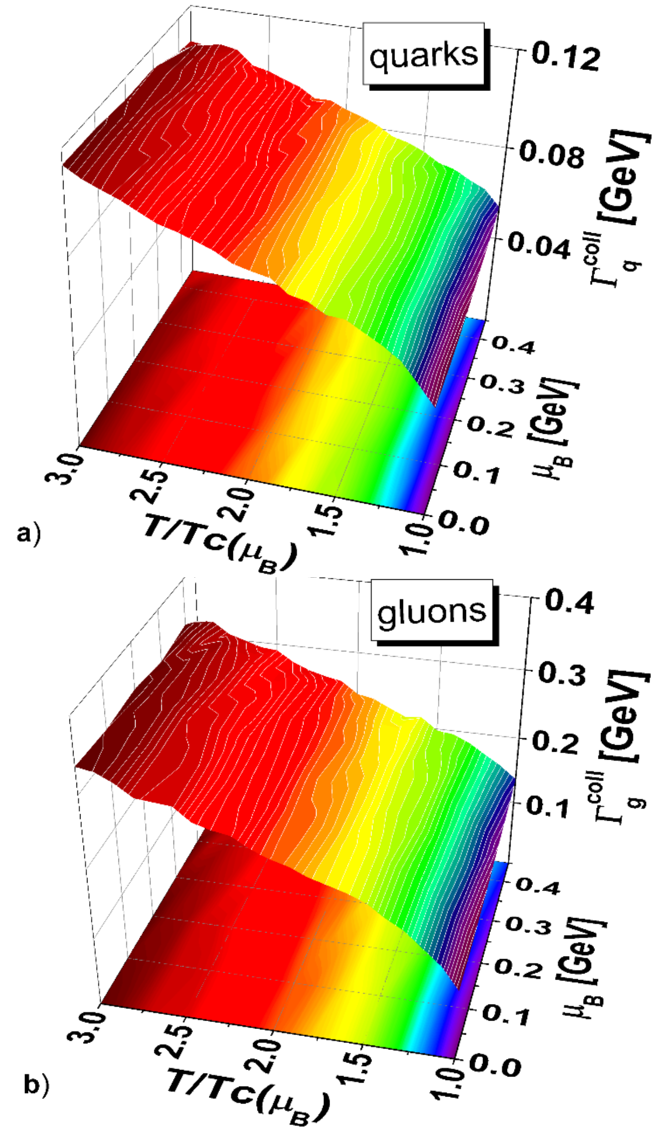

P. Moreau et al., arXiv:1903.10257, PRC (2019)

Transport coefficients: shear viscosity

- **Kubo formalism**

$$\eta^{\rm Kubo}(T,\mu_q) = -\int \frac{d^4p}{(2\pi)^4}\, p_x^2 p_y^2 \sum_{i=q,\bar{q},g} d_i\, \frac{\partial f_i(\omega)}{\partial \omega}\, \rho_i(\omega,\mathbf{p})^2$$

$$= \frac{1}{15T}\int \frac{d^4p}{(2\pi)^4}\, \mathbf{p}^4 \sum_{i=q,\bar{q},g} d_i\, \left((1\pm f_i(\omega)) f_i(\omega)\right) \rho_i(\omega,\mathbf{p})^2$$

- **Relaxation Time Approximation**

$$\eta^{\rm RTA}(T,\mu_q) = \frac{1}{15T}\int \frac{d^3p}{(2\pi)^3} \sum_{i=q,\bar{q},g}$$

$$\left(\frac{\mathbf{p}^4}{E_i^2\ \Gamma_i(\mathbf{p}_i,T,\mu_q)}\, d_i\, \left((1\pm f_i(E_i)) f_i(E_i)\right)\right) + \mathcal{O}(\Gamma_i)$$

Rate Γ (all diagrams for M in the pole mass)
For on-shell case (ρ→δ) Γ=2γ, γ– collisional width

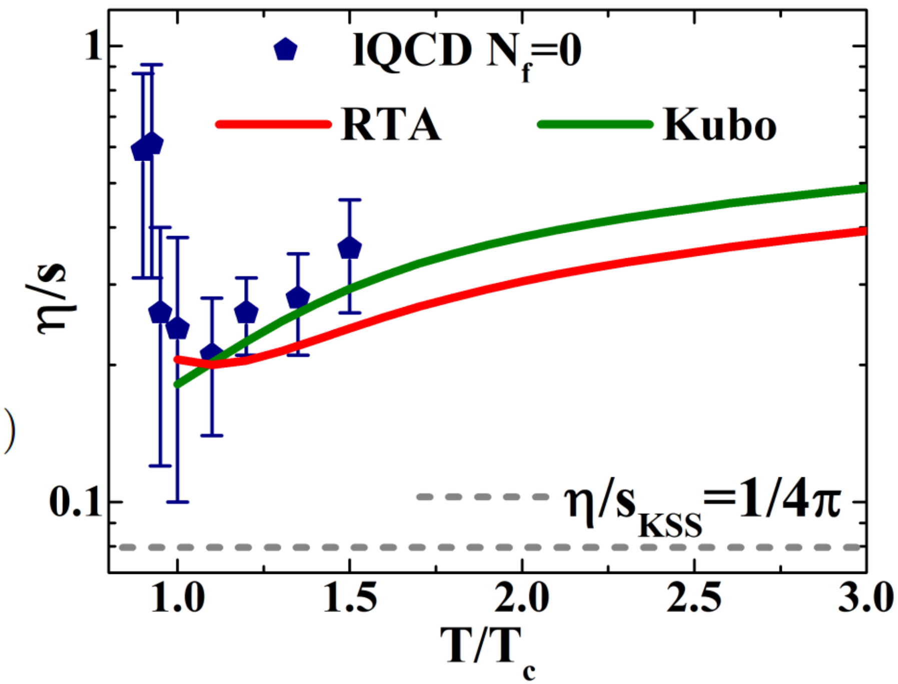

P. Moreau et al., arXiv:1903.10257, PRC (2019)

Transport coefficients: shear viscosity

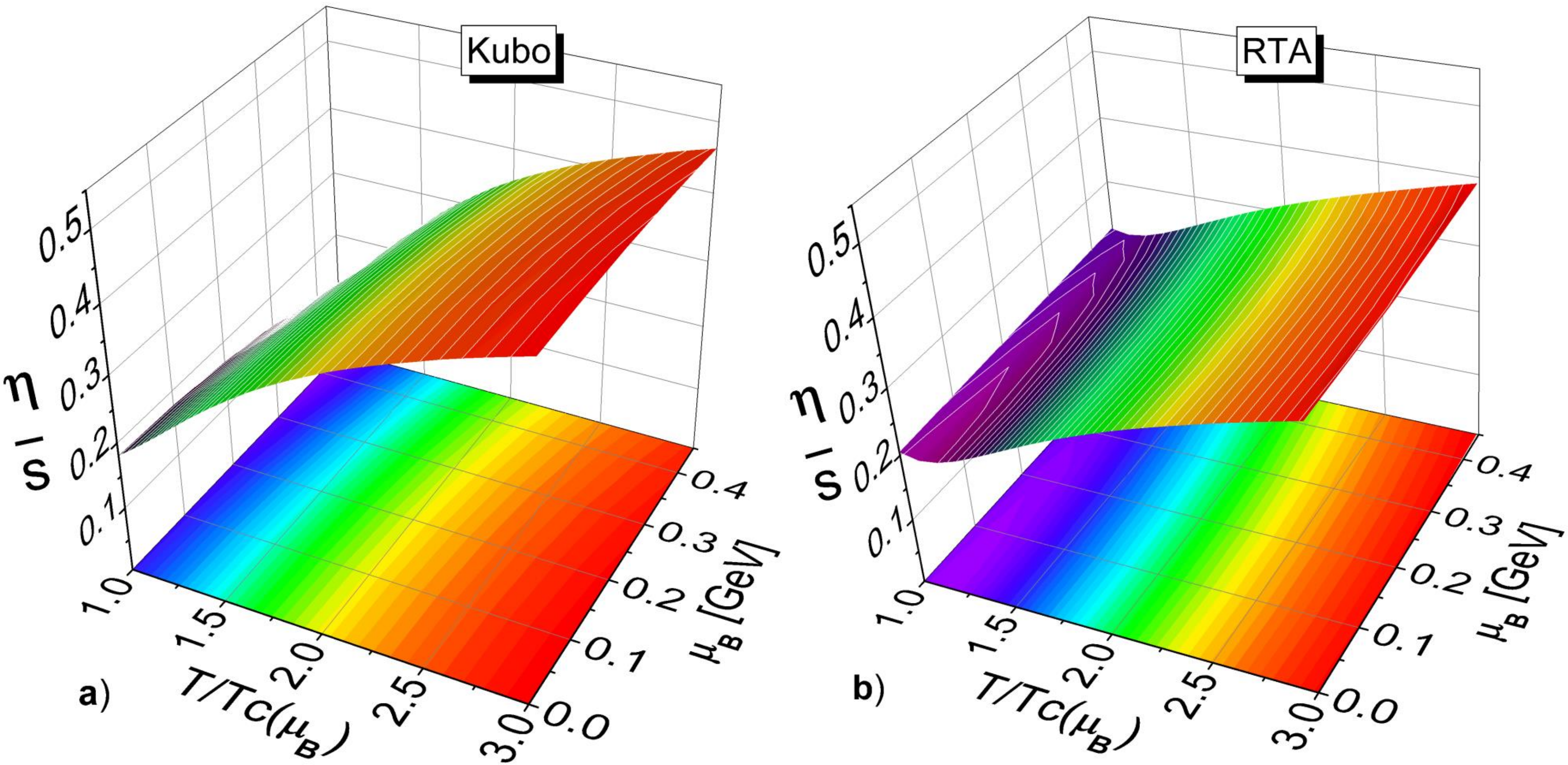

- **Very weak μ_B dependence**

P. Moreau et al., arXiv:1903.10257, PRC (2019)

Transport coefficients: bulk viscosity

➤ **Relaxation Time Approximation**

$$\zeta^{\mathrm{RTA}}(T,\mu_q) = \frac{1}{9T}\int \frac{d^3p}{(2\pi)^3}\sum_{i=q,\bar{q}}$$

$$\left(\frac{\mathbf{p}^4}{E_i^2\;\Gamma_i(\mathbf{p}_i,T,\mu_q)}\; d_i\,((1\pm f_i(E_i))f_i(E_i))\right)[\mathbf{p}^2 - 3c_s^2(E_i^2 - T^2\frac{dm_q^2}{dT^2})]^2$$

from DQPM parametrization

rate

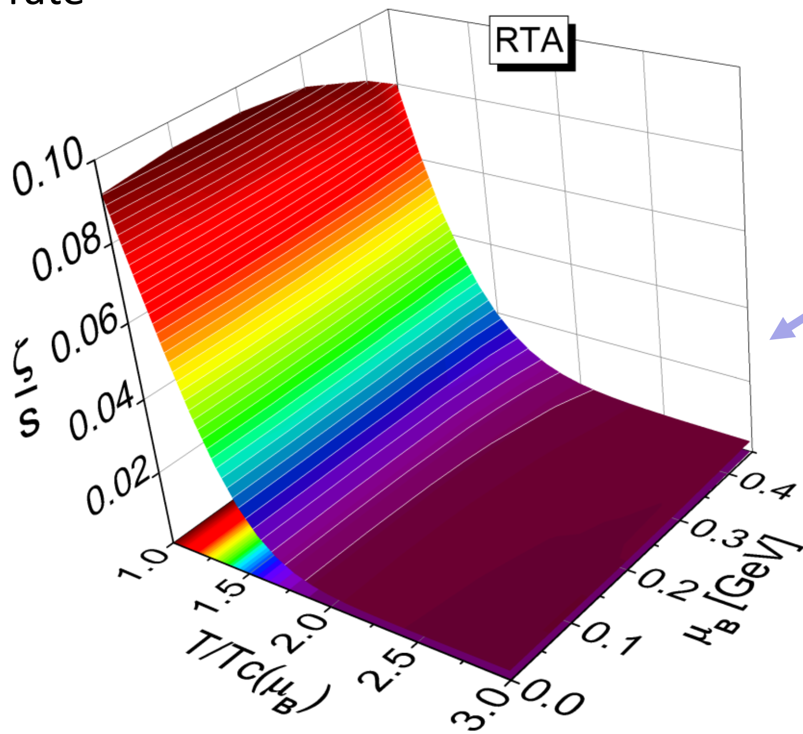

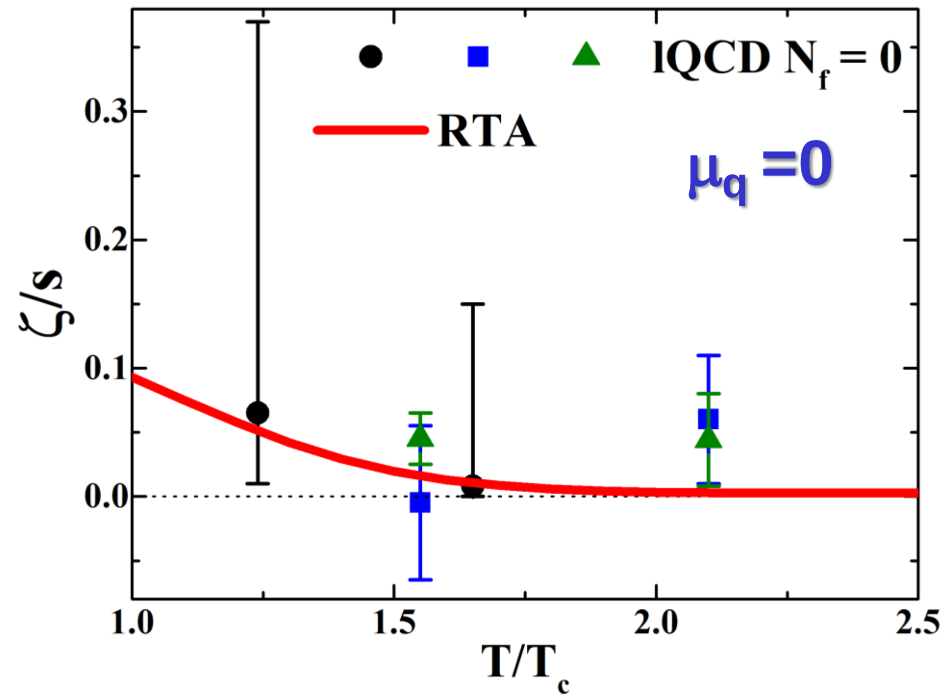

P. Moreau et al., arXiv:1903.10257, PRC (2019)

QGP:
in-equilibrium → off-equilibrium

Parton-Hadron-String-Dynamics (PHSD)

PHSD is a **non-equilibrium microscopic transport approach** for the description of **strongly-interacting hadronic and partonic matter** created in heavy-ion collisions

Dynamics: based on the solution of **generalized off-shell transport equations** derived from Kadanoff-Baym many-body theory

Initial A+A collision

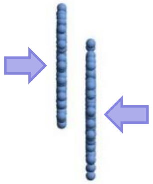

- ❑ **Initial A+A collisions** :
  N+N → string formation → decay to pre-hadrons + leading hadrons

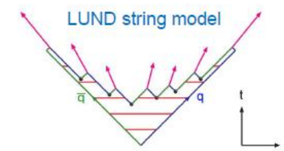

Partonic phase

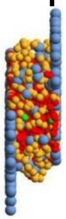

- ❑ **Formation of QGP stage** if local $\varepsilon > \varepsilon_{critical}$:
  dissolution of pre-hadrons → partons

- ❑ **Partonic phase - QGP:**
  QGP is described by the Dynamical QuasiParticle Model (DQPM) matched to reproduce lattice QCD EoS for finite T and μ_B (crossover)

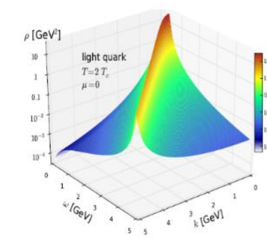

Hadronization

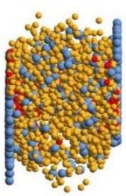

- **Degrees-of-freedom:** strongly interacting quasiparticles: massive quarks and gluons (g,q,q_{bar}) with sizeable collisional widths in a self-generated mean-field potential

- **Interactions:** (quasi-)elastic and inelastic collisions of partons

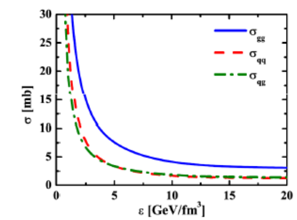

Hadronic phase

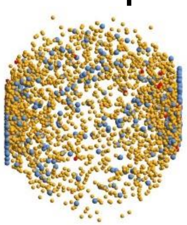

- ❑ **Hadronization** to colorless off-shell mesons and baryons:
  Strict 4-momentum and quantum number conservation

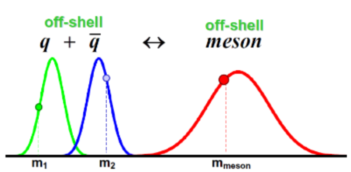

- ❑ **Hadronic phase: hadron-hadron interactions – off-shell HSD**

Extraction of (T, μ_B) in PHSD

- In each space-time cell of the PHSD, the energy-momentum tensor is calculated by the formula: $$T^{\mu\nu} = \sum_i \frac{p_i^\mu p_i^\nu}{E_i}$$

- Diagonalization of the energy-momentum tensor to get the energy density and pressure components expressed in the local rest frame (LRF)

$$T^{\mu\nu} = \begin{pmatrix} T^{00} & T^{01} & T^{02} & T^{03} \\ T^{10} & T^{11} & T^{12} & T^{13} \\ T^{20} & T^{21} & T^{22} & T^{23} \\ T^{30} & T^{31} & T^{32} & T^{33} \end{pmatrix} \Rightarrow \begin{pmatrix} \epsilon^{LRF} & 0 & 0 & 0 \\ 0 & P_x^{LRF} & 0 & 0 \\ 0 & 0 & P_y^{LRF} & 0 \\ 0 & 0 & 0 & P_z^{LRF} \end{pmatrix}$$

For each space-time cell of the PHSD:

- **Calculate the local energy density ε^{PHSD} and baryon density n_B^{PHSD}**
- **use lQCD relations (up to 4th order):**

$$\begin{cases} \dfrac{n_B}{T^3} \approx \chi_2^B(T) \left(\dfrac{\mu_B}{T}\right) + \ldots \\ \Delta\epsilon/T^4 \approx \dfrac{1}{2}\left(T\dfrac{\partial \chi_2^B(T)}{\partial T} + 3\chi_2^B(T)\right)\left(\dfrac{\mu_B}{T}\right)^2 + \ldots \end{cases}$$

➔ **obtain (T, μ_B) by solving the system of coupled equations using ε^{PHSD} and n_B^{PHSD}**

P. Moreau et al., arXiv:1903.10257, PRC (2019)

Extraction of (T, μ_B) in PHSD

For each space-time cell of the PHSD:

- **Correction for the medium anisotropy to extract values for (T, μ_B)**

$$\epsilon^{\text{anis}} = \epsilon^{\text{EoS}} \ r(x)$$

$$P_\perp = P^{\text{EoS}} \ [r(x) + 3xr'(x)]$$

$$P_\parallel = P^{\text{EoS}} \ [r(x) - 6xr'(x)]$$

$$r(x) = \begin{cases} \frac{x^{-1/3}}{2}\left[1 + \frac{x \ \text{arctanh}\sqrt{1-x}}{\sqrt{1-x}}\right] & \text{for } x \leq 1 \\ \frac{x^{-1/3}}{2}\left[1 + \frac{x \ \text{arctan}\sqrt{x-1}}{\sqrt{x-1}}\right] & \text{for } x \geq 1 \end{cases}$$

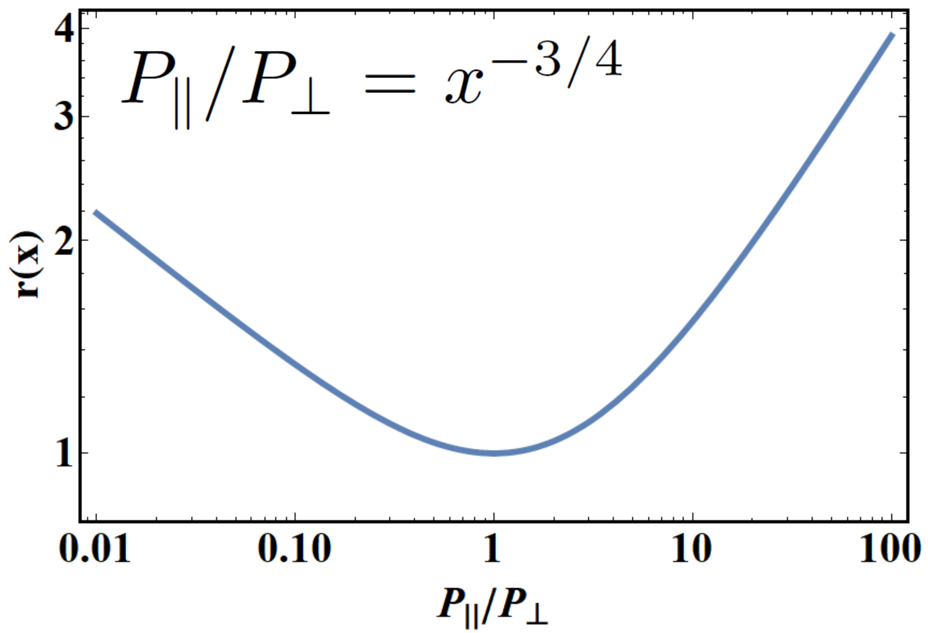

Ryblewski, Florkowski, Phys.Rev. C85 (2012) 064901

- **We have to solve the following system in PHSD:**

$$\begin{cases} \epsilon^{\text{EoS}}(T, \mu_B) = \epsilon^{\text{PHSD}} / r(x) \\ n_B^{\text{EoS}}(T, \mu_B) = n_B^{\text{PHSD}} \end{cases}$$

Done by Newton-Raphson method

T, P in HIC ($\sqrt{s_{NN}} = 200$ GeV)

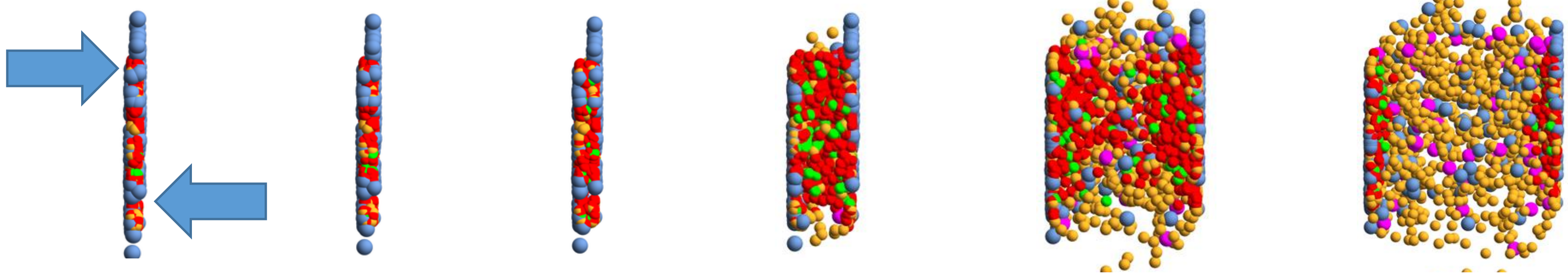

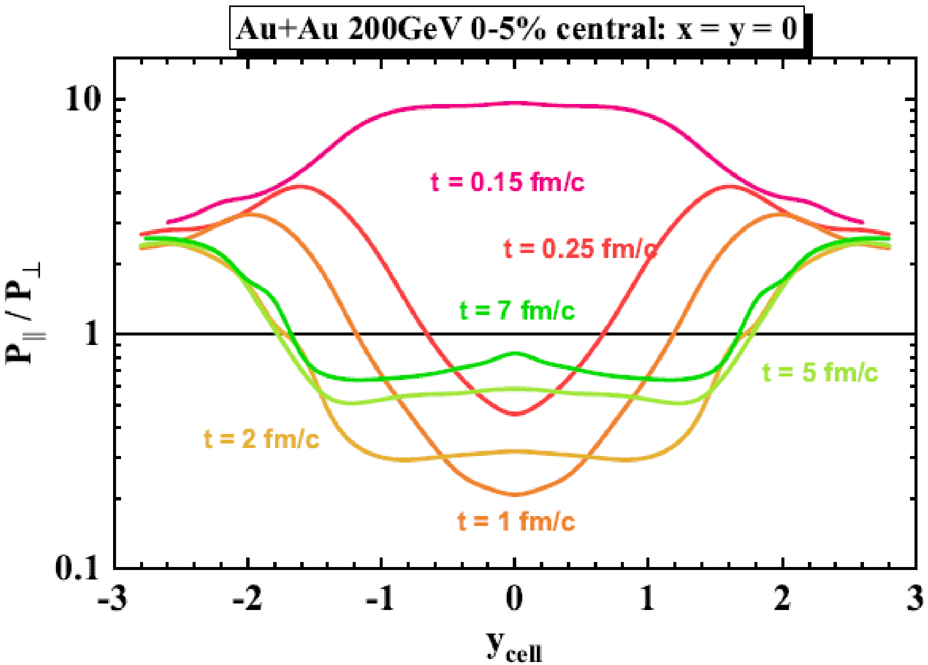

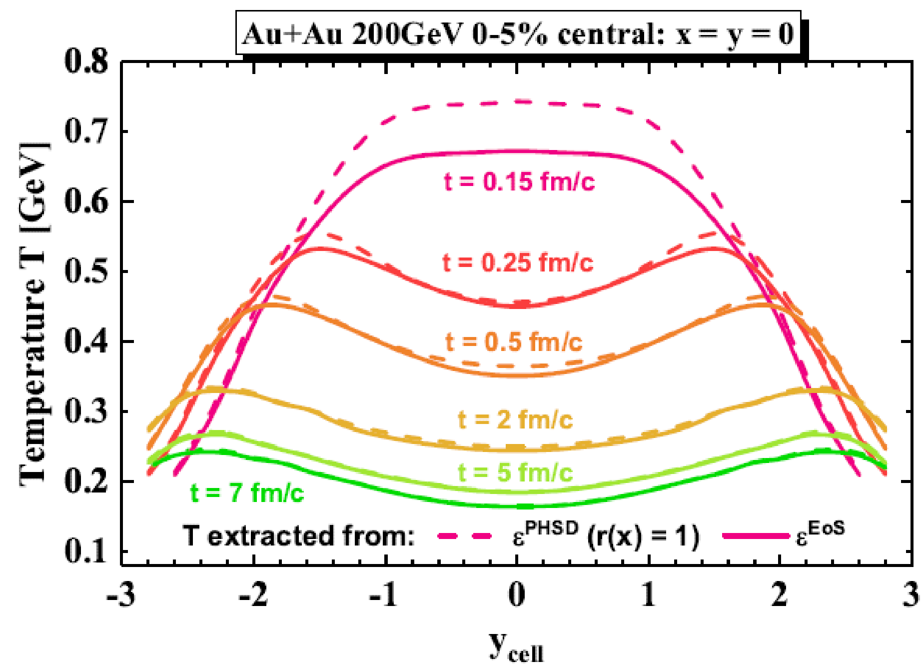

Cf. talk by Takeshi Kodama

P. Moreau et al., arXiv:1903.10257, PRC (2019)

T, P in HIC ($\sqrt{s_{NN}} = 200$ GeV)

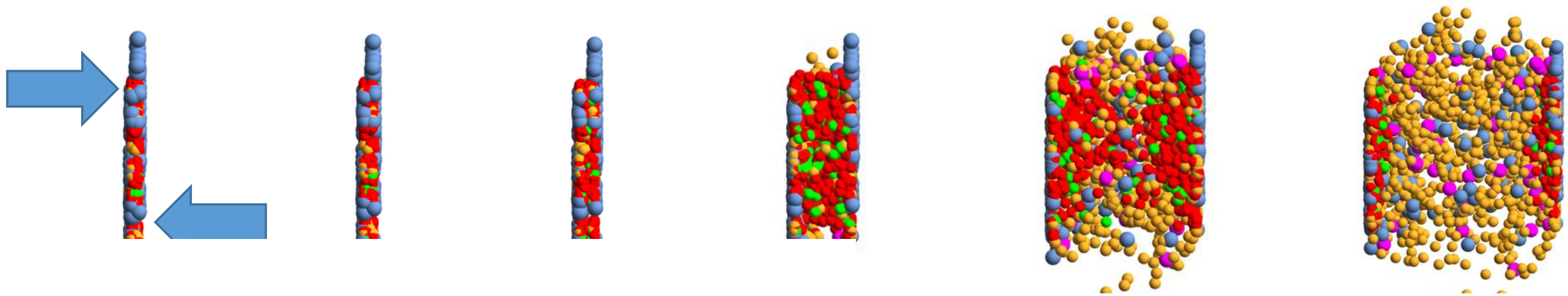

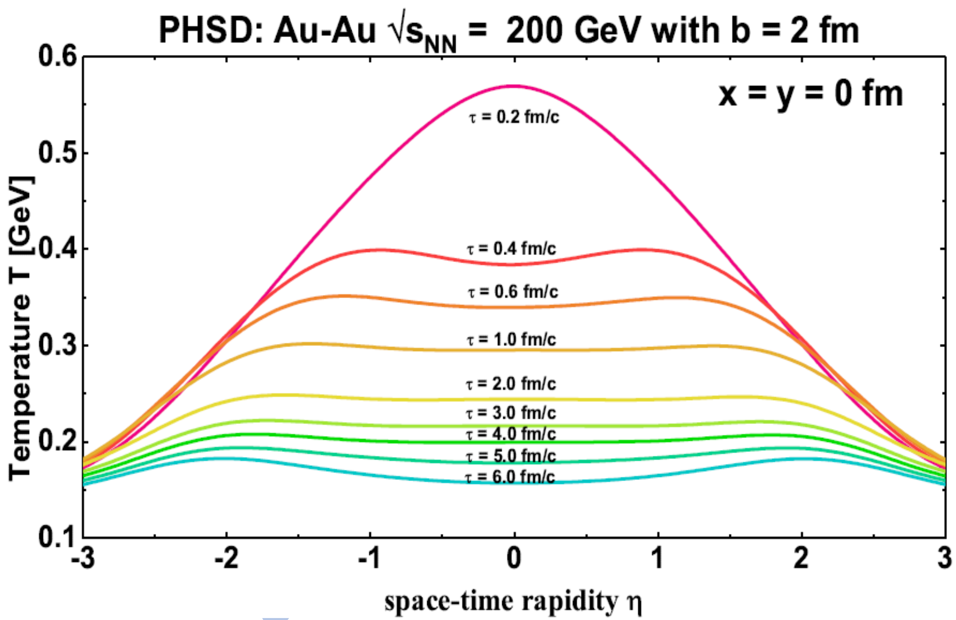

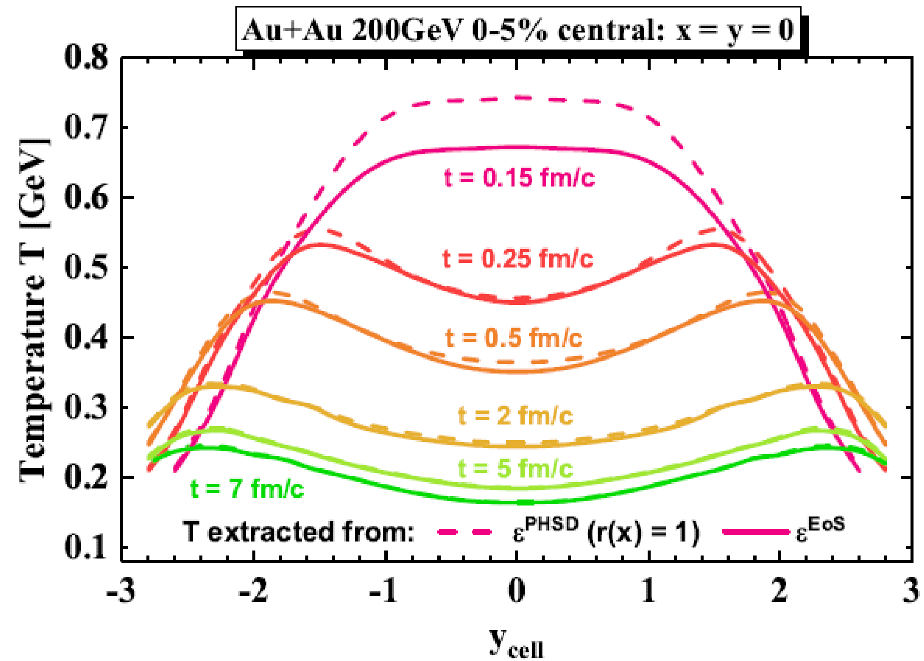

Milne coordinates (τ,x,y,η) : temperature profile - almost boost-invariant

P. Moreau et al., arXiv:1903.10257, PRC (2019)

Illustration for HIC ($\sqrt{s_{NN}} = 19.6$ GeV)

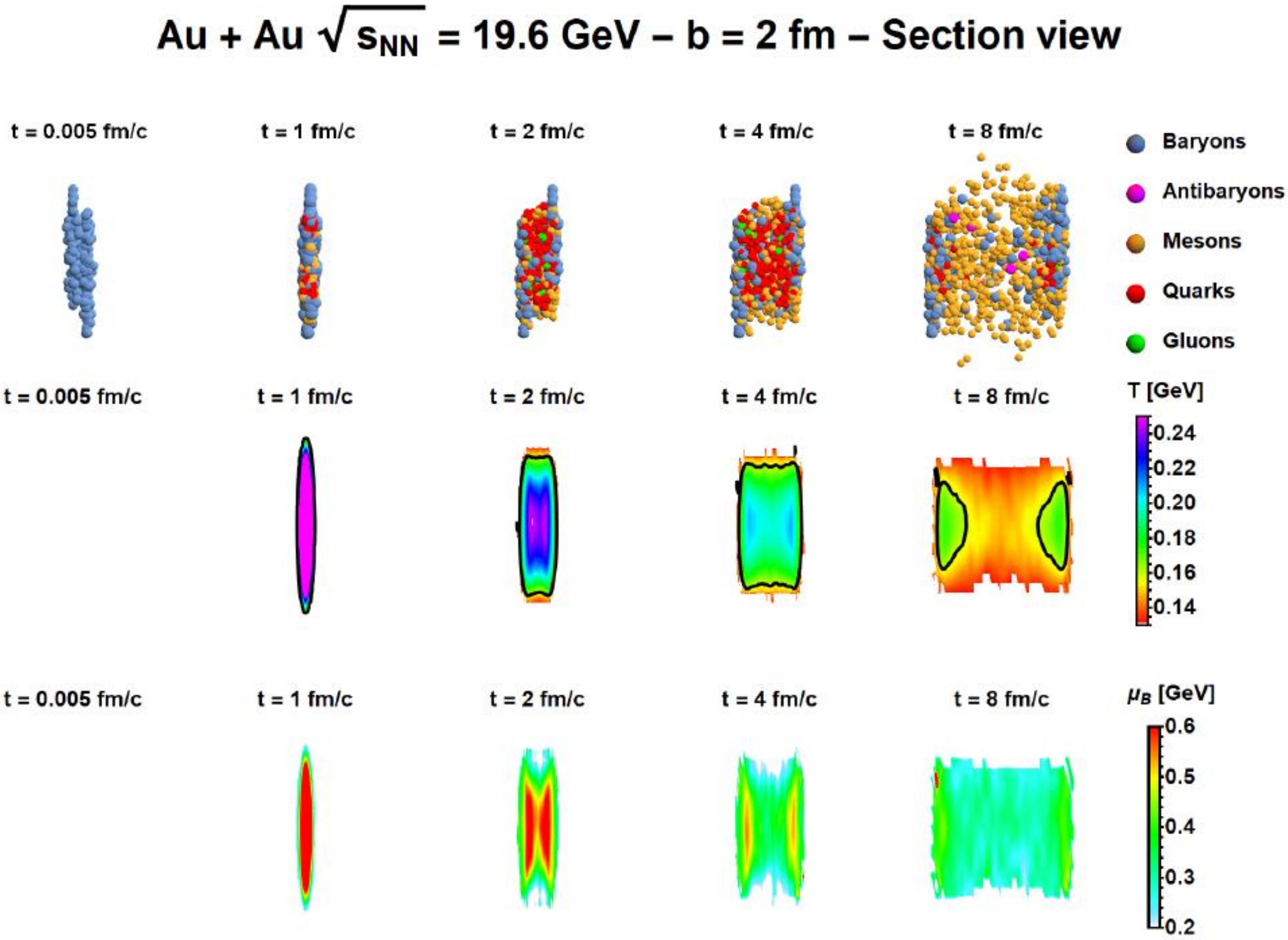

Illustration for HIC ($\sqrt{s_{NN}} = 17$ GeV)

The temperature profile in (x; y) **Baryon chemical potential profile in (x;y)**
at midrapidity ($|y_{cell}|$< 1) at 1 and 4 fm/c

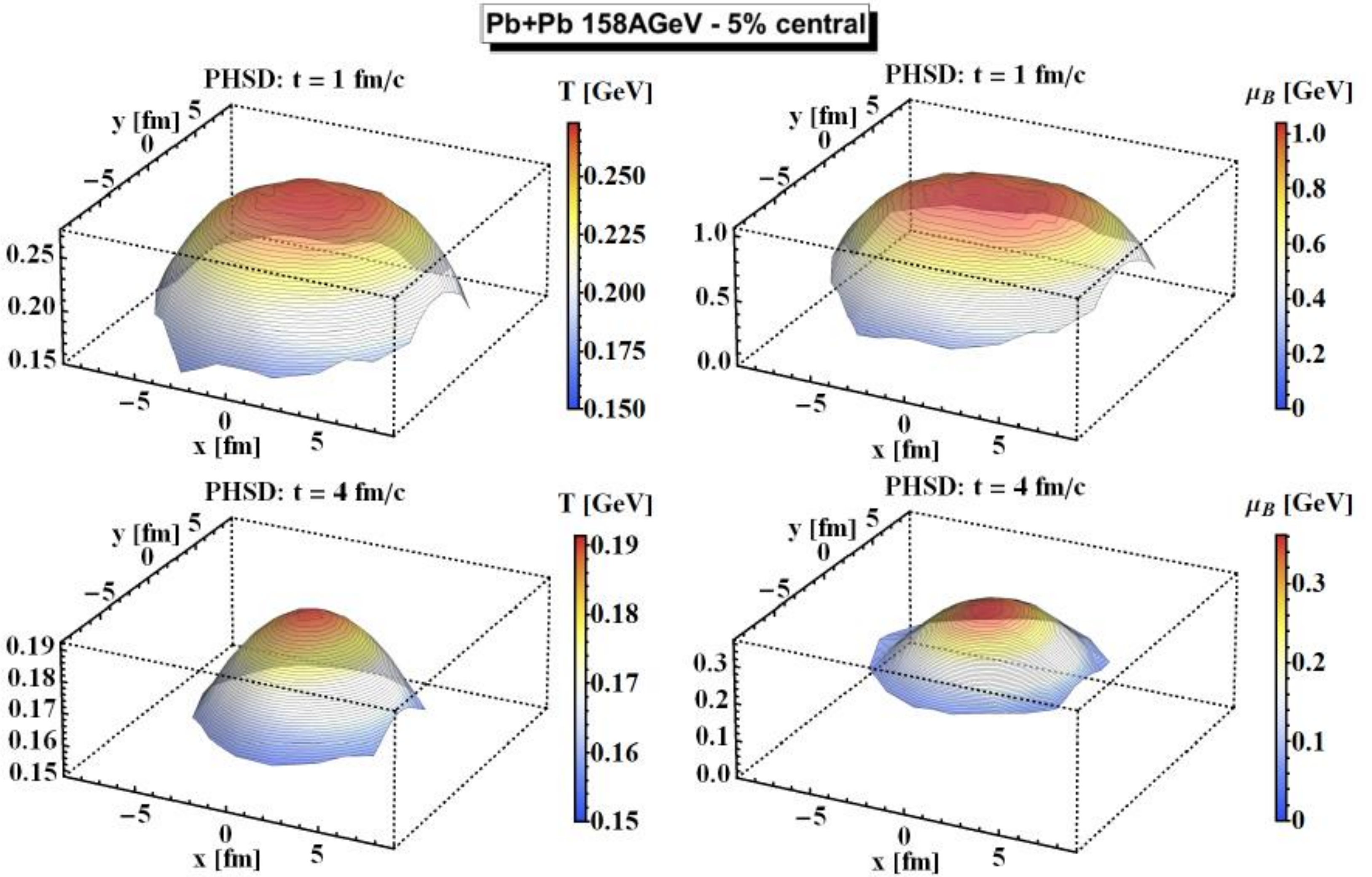

P. Moreau et al., arXiv:1903.10257, PRC (2019)

Illustration for HIC ($\sqrt{s_{NN}} = 17$ GeV)

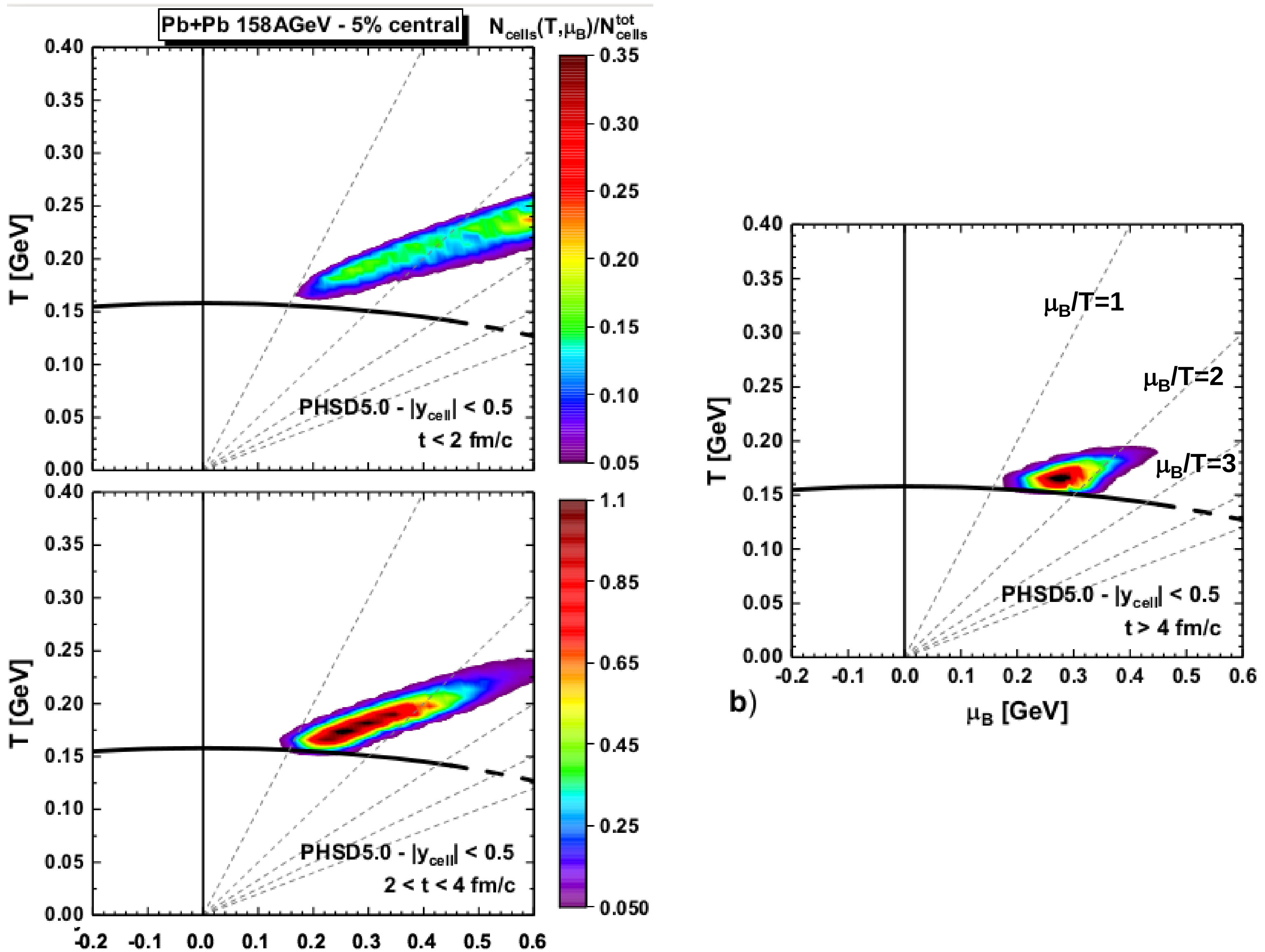

P. Moreau et al., arXiv:1903.10257, PRC (2019)

Traces of the QGP at finite μ_q in observables
in high energy heavy-ion collisions

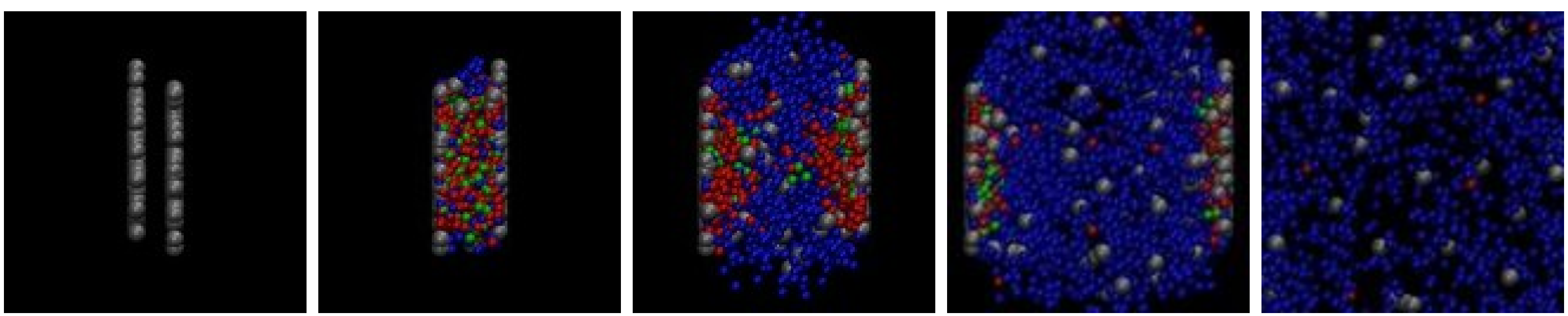

Results for HIC

- **Comparison between three different results:**

  1) **PHSD 4.0 : only $\sigma(T)$ and $\rho(T)$**
  2) **PHSD 5.0 : with $\sigma\left(\sqrt{s}, T, \mu_B = 0\right)$ and $\rho(T, \mu_B = 0)$**
  3) **PHSD 5.0 : with $\sigma\left(\sqrt{s}, T, \mu_B\right)$ and $\rho\ (T, \mu_B)$**

ρ–spectral function

➔ (mass and width)

Results for HIC ($\sqrt{s_{NN}} = 200$ GeV)

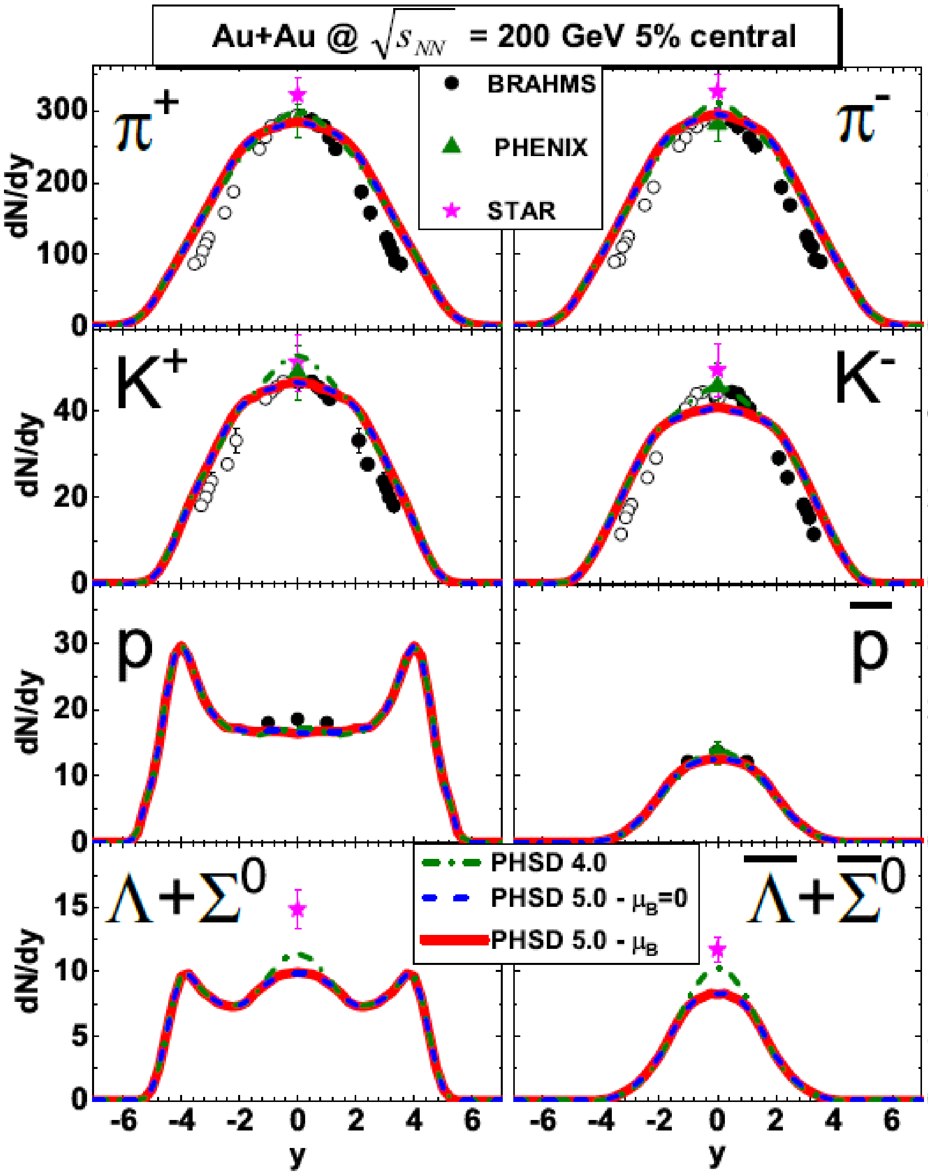

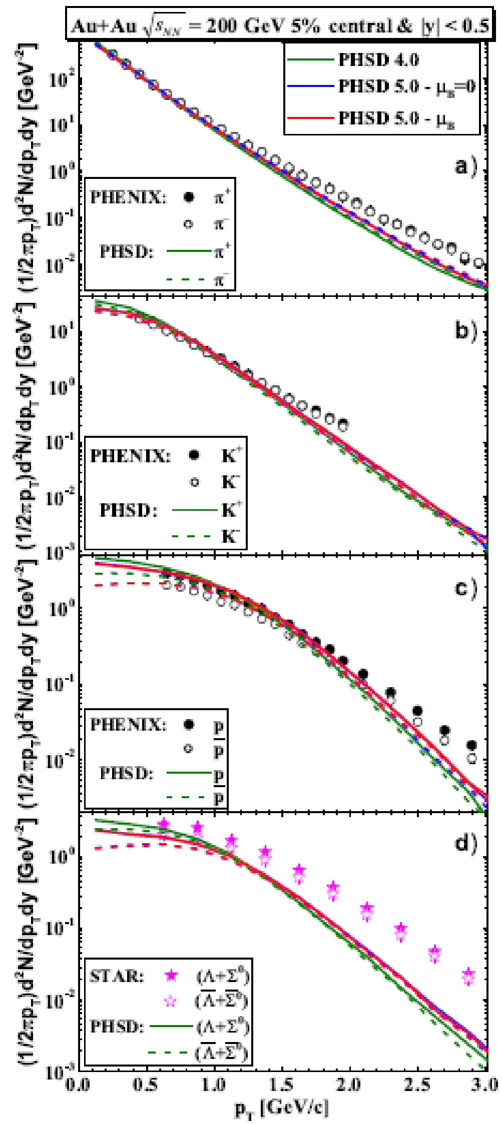

P. Moreau et al., arXiv:1903.10257, PRC (2019)

Results for HIC ($\sqrt{s_{NN}} = 17$ GeV)

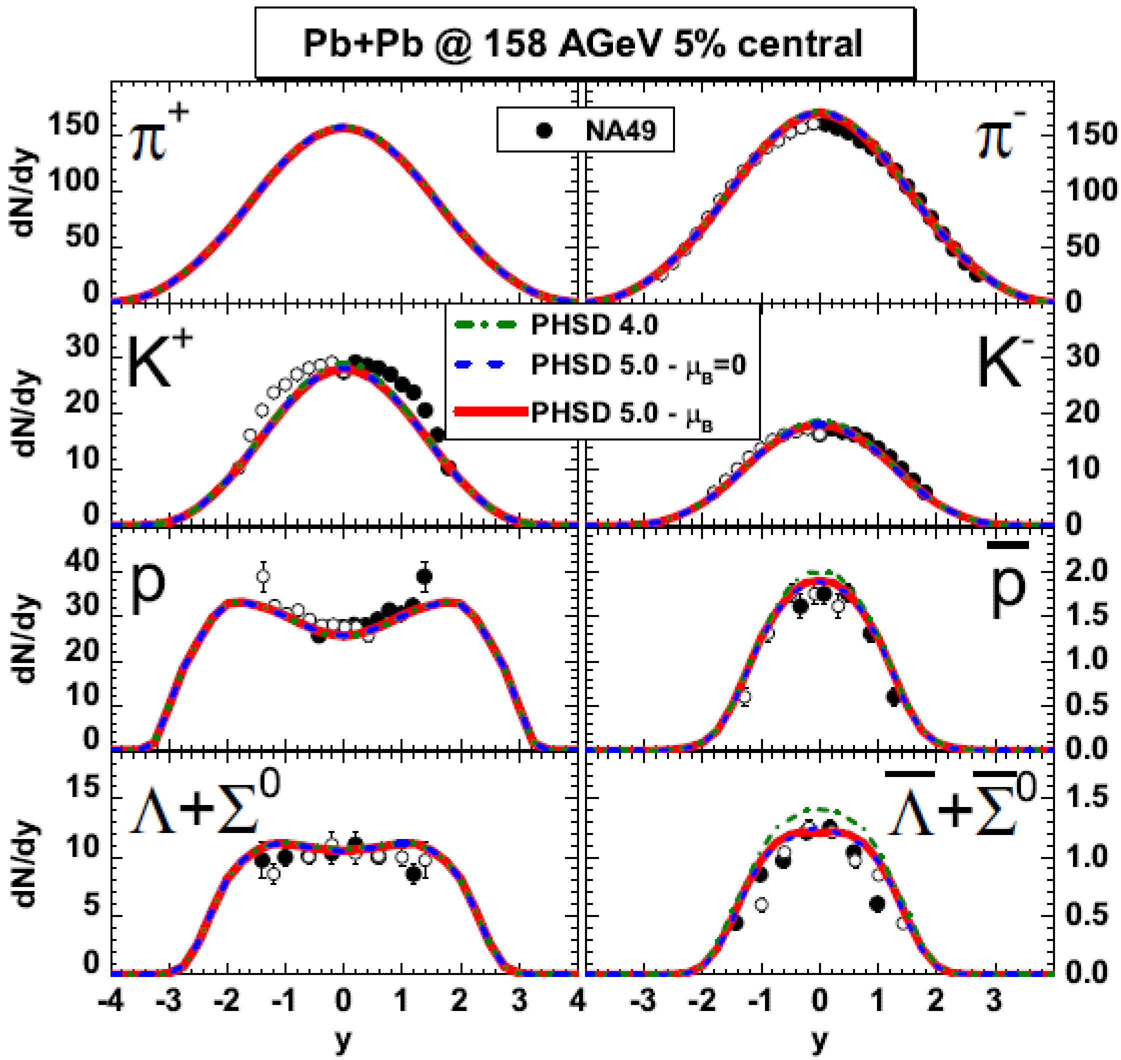

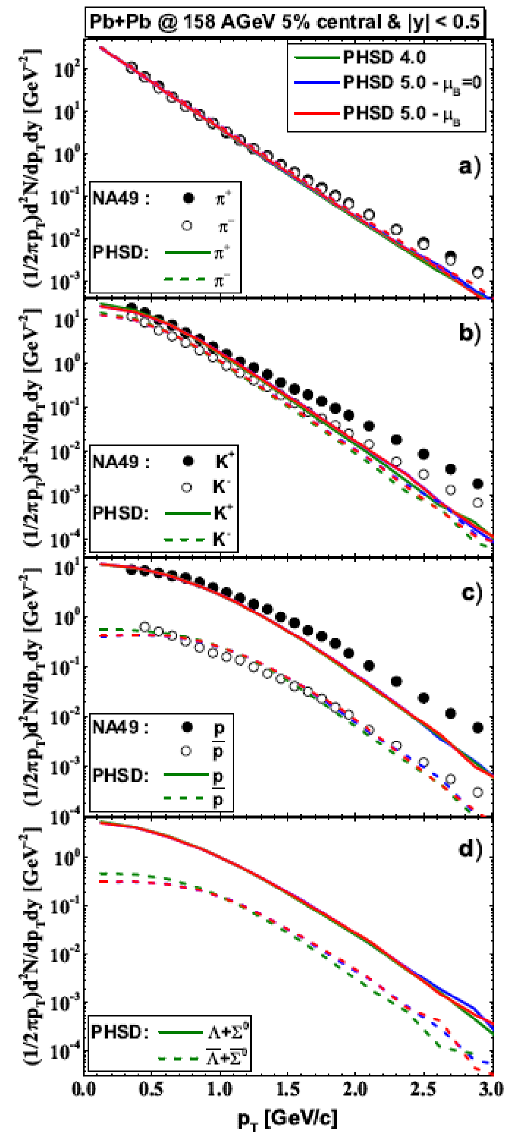

P. Moreau et al., arXiv:1903.10257, PRC (2019)

Results for HIC ($\sqrt{s_{NN}} = 7.6$ GeV)

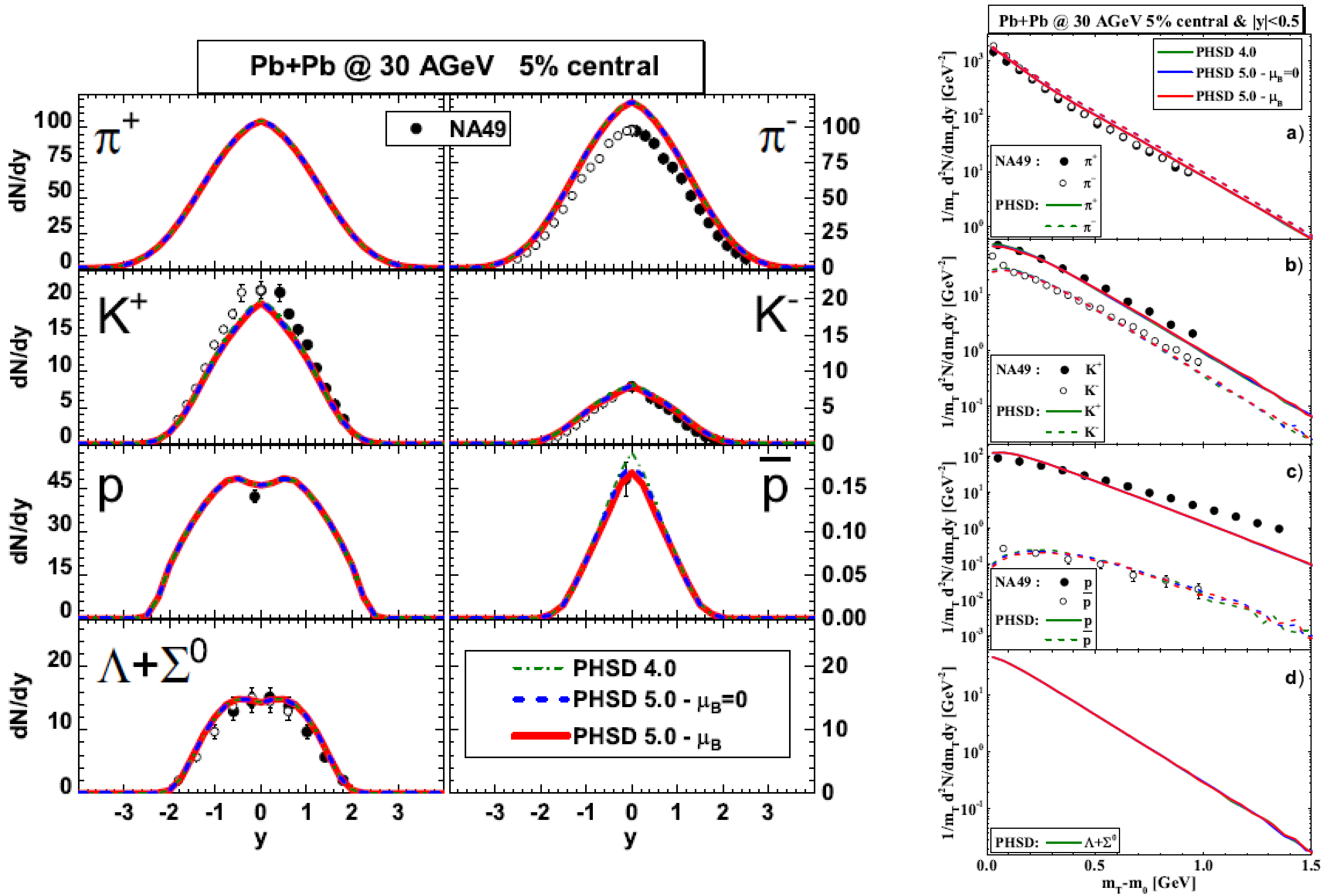

P. Moreau et al., arXiv:1903.10257, PRC (2019)

Results for HIC ($\sqrt{s_{NN}} = 4.86$ GeV)

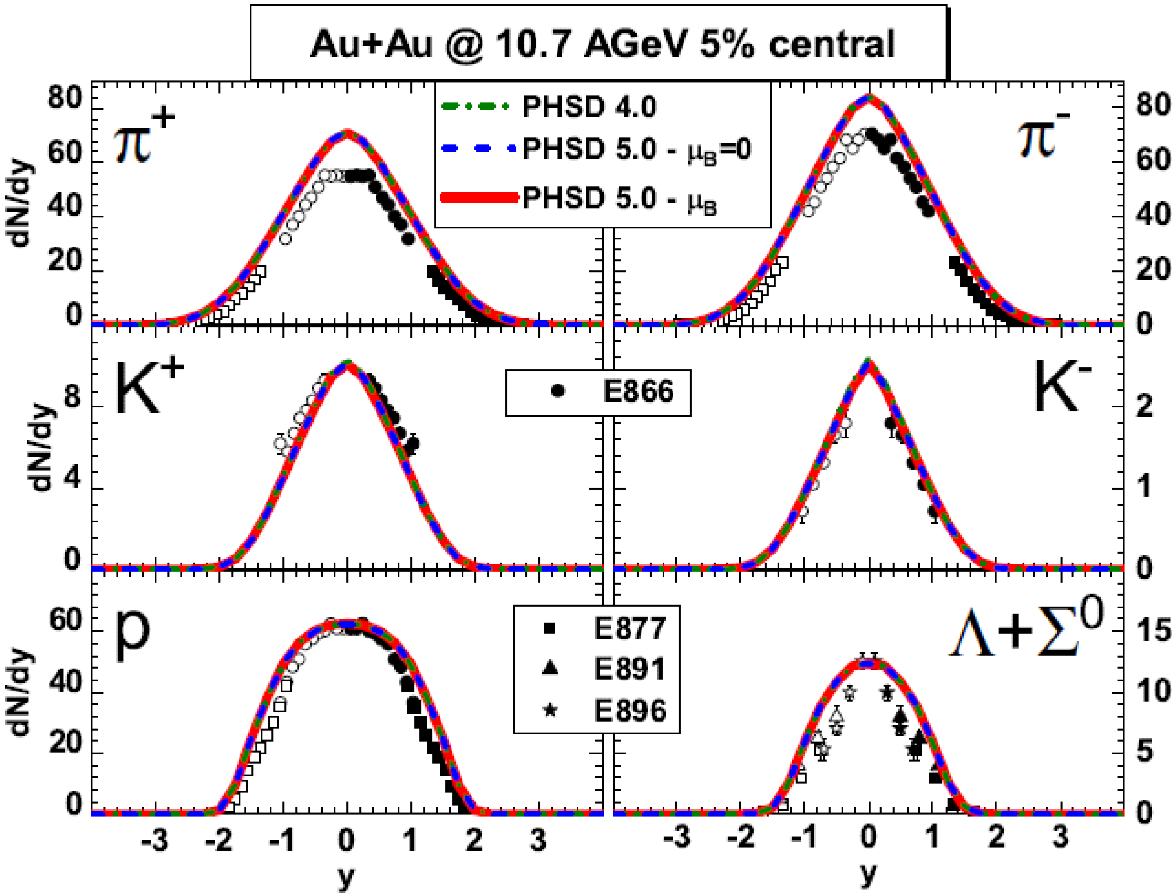

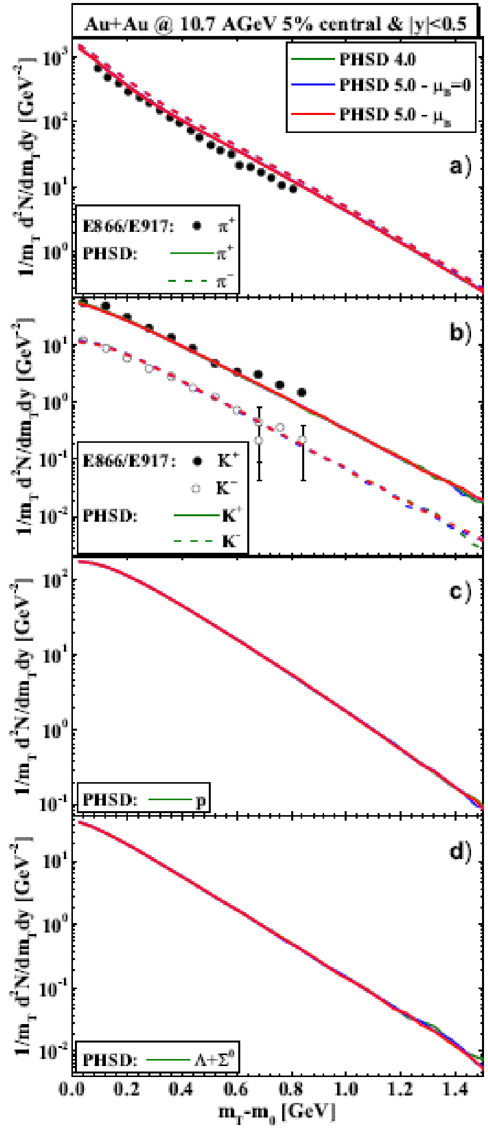

P. Moreau et al., arXiv:1903.10257, PRC (2019)

Results for assymetric systems

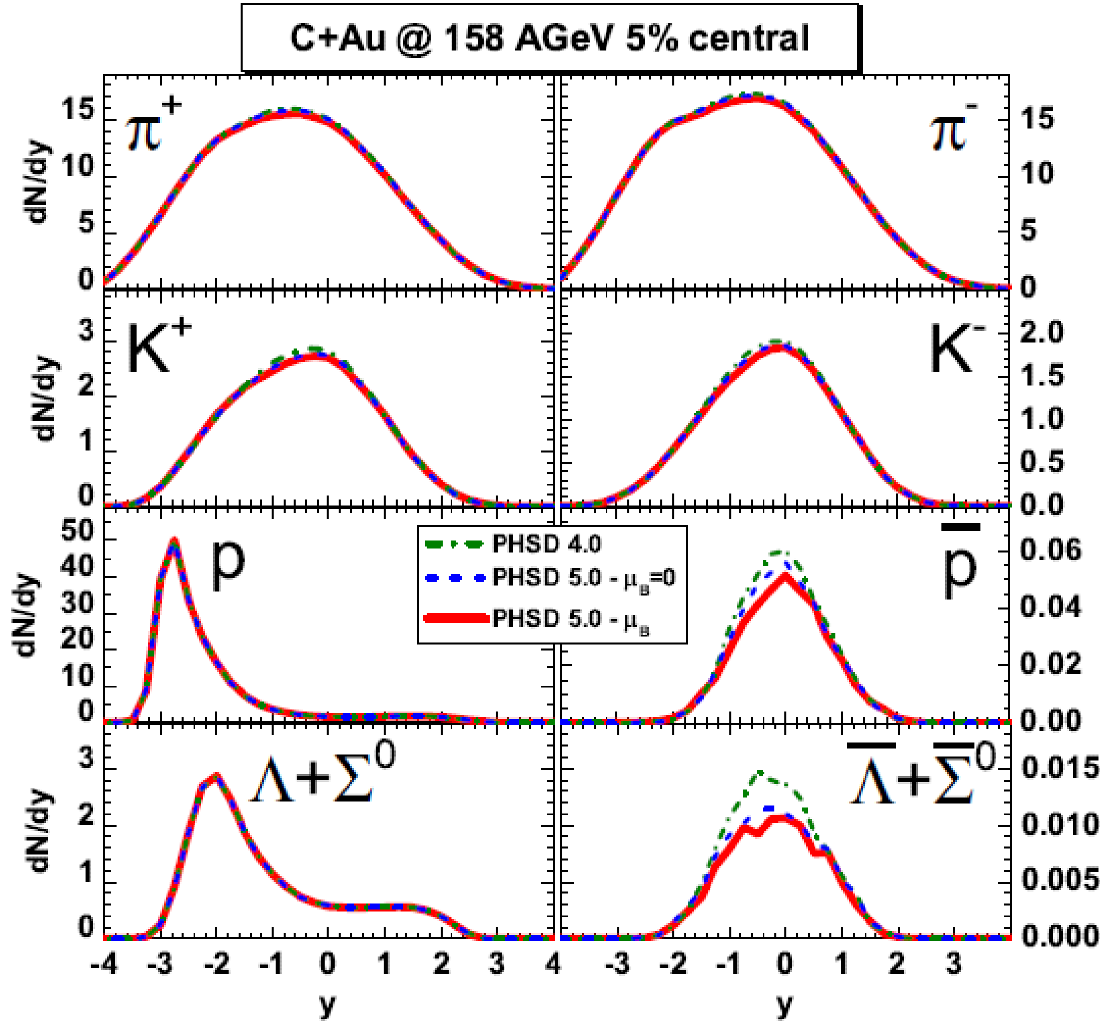

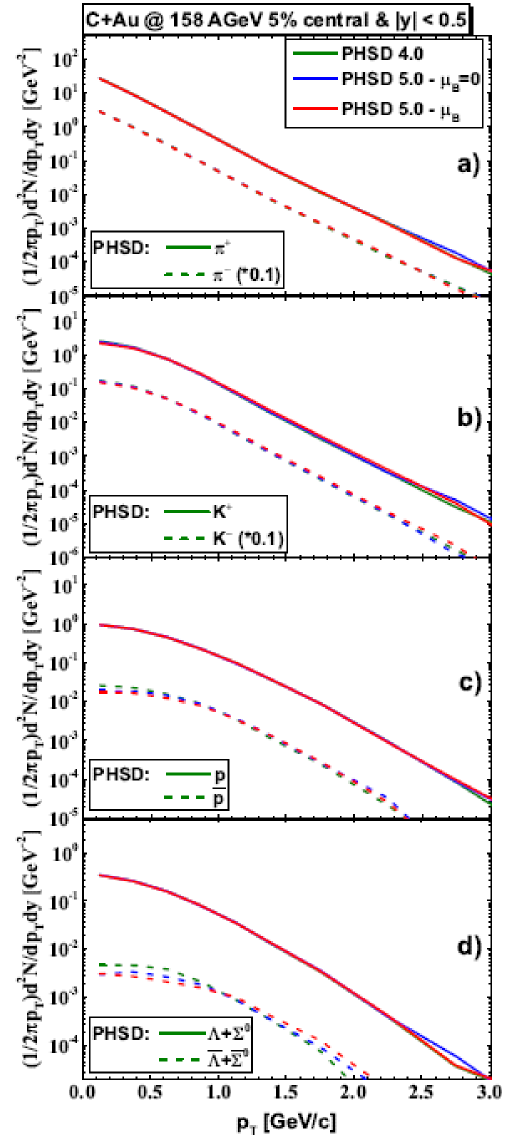

P. Moreau et al., arXiv:1903.10257, PRC (2019)

Summary / Outlook

- (T, μ_B)-dependent cross sections and masses/widths of quarks and gluons have been implemented in PHSD
- High-μ_B regions are probed at low $\sqrt{s_{NN}}$ or high rapidity regions
- But, QGP fraction is small at low $\sqrt{s_{NN}}$:

  ➔ no effects seen in bulk observables

- **Outlook:**
  - Study more sensitive probes to finite-μ_B dynamics
  - More precise EoS finite/large μ_B
  - Possible 1[st] order phase transition at large μ_B?!